The Role of ALS8-linked VAMP-associated Protein B (VAPB) in *Caenorhabditis elegans* Motor Neurons

Wendy W. Zhang

Thesis submitted to the
Faculty of Graduate and Postdoctoral Studies
in partial fulfillment of the requirements
for the Master of Science degree in Neuroscience

Department of Cellular and Molecular Medicine

Faculty of Medicine

University of Ottawa

ABSTRACT

Amyotrophic Lateral Sclerosis (ALS) is a fatal, late-onset, progressive neurodegenerative disease. A familial form of ALS, autosomal dominant ALS8, is characterized by a mutation in an ER membrane protein, VAPB. To characterize the role of VAPB in motor neurons, two *C. elegans* models were generated: one expressing human VAPB-P56S and another with the knockdown of *C. elegans* VAPB ortholog, VPR-1. Overexpression of human VAPB in DA neurons caused backward locomotion defects, enhanced vulnerability to oxidative stress and premature neuronal death. Knockdown of *vpr-1* in *C. elegans* recapitulated the loss of protein function believed to be associated with human cases of ALS8. It caused backward locomotion defects, such as uncoordination and slowed rates of movement, as well as age-dependent motor neuronal death. In both models, DA6 and DA7 were the most vulnerable motor neurons. Because of the unexpected developmental defects associated with the VAPB transgenic model, the knockdown of *vpr-1* may be a better model to recapitulate the human disease. This model provides further support that ALS8 pathogenesis is due to a loss of VAPB protein function and can also be used to test drugs or treatments that may delay the onset of neuronal death.

TABLE OF CONTENTS

LIST OF TABLES

LIST OF FIGURES

LIST OF ABBREVIATIONS

ALS	Amyotrophic Lateral Sclerosis
ATP	Adenosine Triphosphate
BMP	Bone Morphogenetic Protein
CCD	Coiled-Coil Domain
cDNA	Complementary Deoxyribonucleic Acid
CHO	Chinese Hamster Ovary
CNS	Central Nervous System
DA	'Dorsal A' motor neuron
DB	'Dorsal B' motor neuron
dsRNA	Double-stranded RNA
DTT	Dithiothreitol
dVAP	*Drosophila* VAP ortholog
EphR	Ephrin Receptor
ER	Endoplasmic Reticulum
ERGIC	ER-Golgi Intermediate Compartment
fALS	Familial ALS
FFAT	Two Phenylalanines in an Acidic Tract
FUDR	5'flurodeoxyuridine
GFP	Green Fluorescent Protein
HDL	High-Density Lipoprotein
HSP	Heat Shock Protein
iPSC	Induced Pluripotent Stem Cell
LDL	Low-Density Lipoprotein
mRNA	Messenger RNA
MSP	Major Sperm Protein
NE	Nuclear Envelope
NGM	Nematode Growth Media
Nups	Nucleoporins
OP50	*Escherichia coli* OP50
ORP	Oxysterol Binding Protein-Related Protein
OSBP	Oxysterol Binding Protein
PCR	Polymerase Chain Reaction
RDE-1	*C. elegans* Argonaute protein
rER	Rough Endoplasmic Reticulum
RNA	Ribonucleic Acid
RNAi	RNA-mediated interference
sALS	Sporadic ALS

sHSP	Small Heat Shock Protein
siRNA	Small Interfering RNA
TDP-43	TAR-DNA binding protein-43
TMD	Transmembrane Domain
UPR	Unfolded Protein Response
VAMP	Vesicle-Associated-Membrane Protein
VAPB	VAMP-associated protein B
VPR-1	*C. elegans* VAP ortholog
WT	Wildtype
XO	Male *C. elegans*
XX	Hermaphrodite *C. elegans*

ACKNOWLEDGEMENTS

I would like to acknowledge and thank my supervisor, Dr. John Ngsee, for taking a chance and believing in me years ago by welcoming me into his lab fresh out of high school through the Undergraduate Research Scholarship program. These past several years have taught me tremendously and have shaped my work ethic, critical thinking and overall appreciation for science and discovery. You have continuously inspired me to take every opportunity to learn and have provided a great learning environment for all of us. Thank you for all your guidance and encouragement, for sharing your knowledge, and for your constant support and patience.

I would also like to extend my sincere thanks to Dr. Antonio Colavita, who has accepted me into his *C. elegans* lab over the last couple of years and has been there with technical support and guidance in the lab and on my thesis advisory committee. I am also very grateful for Dr. Mario Tiberi for being on my thesis advisory committee and for always being willing to share his expertise and helpful advice.

Most of all, thank you to my lab mates and friends for being the reinforcement I needed over the years. I have been very fortunate to work with and get to know a great group of people, including Angie, Kalina, Duvinh, Jess, Allana, Tony, Derek, Heather, Avni, Clare, Rachel, and Jiravat from my lab, along with Cristina, Dave, Matt, Aysha, Ding, and Jeffrey from the Colavita lab. You have become some of my closest friends and have made these years fly by. Thank you to my family as well for all the support, understanding and acceptance of the lab becoming my second home. This would not have been possible without all of you.

INTRODUCTION

Amyotrophic Lateral Sclerosis is an adult-onset neurodegenerative disease

Amyotrophic Lateral Sclerosis (ALS), also known as Lou Gehrig's disease, is a late-onset, progressive neurodegenerative disease that results in a rapid loss of upper and lower motor neurons in the cortex, brain stem, and spinal cord, leading to increasing skeletal muscle atrophy. Spasticity, fasciculation, dysarthria, dysphagia and limb-weakness are common clinical features of ALS (Kuhnlein et al., 2008). As voluntary muscles weaken and deteriorate, this fatal disease not only leaves the senses unaffected, but the intellect may remain unaltered as well before leading to death by respiratory failure within two to five years of symptom-onset. ALS affects males more often than females and people are generally diagnosed in their late 40-60s (Boillee et al., 2006). Every year, approximately two people per 100,000 are diagnosed with ALS, and currently, 2500-3000 Canadians live with this fatal motor neuron disease (ALS Society of Canada).

First defined over 145 years ago by French neurobiologist and clinician, Jean-Martin Charcot, autopsy studies and clinical observations led Charcot and his team to discover lesions within the lateral column and anterior horn of the spinal cord, resulting in progressive muscle paralysis. He coined the name "Amyotrophic Lateral Sclerosis" in 1874 (Kumar et al., 2011), which translates to "an absence of muscle nourishment and hardening of the (lateral) spinal cord". Although initially described by Charcot as non-hereditary, in the 1950s, Kurland and Mulder reported 58 patients with 10% of them having familial ALS (Kurland and Mulder, 1955a; Kurland and Mulder, 1955b). Both

sporadic ALS (sALS) and familial ALS (fALS) have similar pathological hallmarks, and while 90% of ALS cases today are sporadic (sALS), advances in genetics have linked over ten genes to familial cases of ALS (fALS) (Table 1). Unfortunately, although progress has been made in palliative care for those living with this debilitating disease, further therapeutic options have yet to be discovered and ALS still remains an incurable condition.

Table 1. Genes associated with Amyotrophic Lateral Sclerosis

Data reproduced from (Al-Chalabi and Hardiman, 2013; Boillee et al., 2006) and OMIM.org.

Disease	Gene	Gene name	Onset	Hereditary
ALS1	*SOD1*	Superoxide dismutase 1	Adult	Dominant
ALS2	*ALS2*	Alsin	Juvenile	Recessive
ALS3	Unknown	Unknown	Adult	Dominant
ALS4	*SETX*	Senataxin	Juvenile	Dominant
ALS5	*SPAST*	Spastin	Juvenile	Recessive
ALS6	*FUS*	Fused in sarcoma	Adult	Dominant
ALS7	Unknown	Unknown	Adult	Dominant
ALS8	*VAPB*	VAMP-associated protein B	Adult	Dominant
ALS9	*ANG*	Angiogenin	Adult	Dominant
ALS10	*TARDBP*	TAR DNA binding protein	Adult	Dominant
ALS-FTD 2	*C9orf72*	Chromosome 9 open reading frame 72	Adult	Dominant

Familial ALS8 is characterized by VAPB-P56S

In 2004, Nishimura and colleagues report 26 members of a three generation Caucasian Brazilian family affected by an adult-onset, autosomal dominant motor neuron disease with clinical diagnoses consistent of ALS. This led to the discovery of a novel locus at 20q13.33 linked to ALS, deemed familial ALS8 (Nishimura et al., 2004a). All patients of this large Brazilian family of Portuguese descent, together with six additional affected families for a total of over 200 patients, have a single missense mutation in the vesicle-associated membrane protein (VAMP)/synaptobrevin-associated membrane protein B gene (VAPB) causing a C→T substitution at the 56th residue of the gene (VAPB-P56S) (Nishimura et al., 2004b). Recently, in 2010, ALS8 was found to not be restricted to South America with the identification of a German (Funke et al., 2010) and a Japanese (Millecamps et al., 2010) with the same mutation.

Despite being defined by the same mutation, ALS8 has a variable clinical course. Although both males and females appear to be affected equally and all patients experience cramps, fasciculation, and limb weakness, some ALS8 patients may face a rapid and severe progression whereas others experience a slow progression that takes decades (Mitne-Neto et al., 2011) after the initial onset of disease between 25-55 years of age.

VAMP-associated protein B (VAPB) and VAPB-P56S

ALS8 is a heterogeneous, autosomal dominant form of familial ALS characterized by a single missense mutation, VAPB-P56S. This missense mutation at the 166th nucleotide causes a substitution of the conserved proline for a serine at the 56th

residue (P56S) of VAPB. VAPB is a member of the vesicle-associated membrane protein (VAMP) -associated protein family, which was originally described and identified in 1995 as VAP-33 in *Aplysia californica* (Skehel et al., 1995). VAMP-associated proteins (VAP) are type II integral membrane proteins that assist in the overall function of the endoplasmic reticulum (ER) and Golgi apparatus. This includes roles in vesicle-trafficking, neurotransmitter release, ER-to-Golgi apparatus transport, structural regulation of the ER as well as intra-Golgi transportation (Suzuki et al., 2009). Localized in the ER and ER-Golgi intermediate compartment (ERGIC), VAMP-associated proteins are phylogenetically conserved and various VAP orthologs exist across assorted species from yeast to mammals, such as VPR-1 in *Caenorhabditis elegans* (Mitne-Neto et al., 2011).

There are 2 VAP genes in human, designated VAPA and VAPB. VAPA and VAPB share a similar protein structure with 76% identity and are expressed ubiquitously, which suggests that their function is required by all cells (Nishimura et al., 1999). VAPB, which is linked to ALS8, is comprised of three structural domains. The highly conserved amino (N)-terminal major sperm protein (MSP) domain encompasses the first 124 residues. The central domain forms a coiled/coil protein-protein interaction motif due to its amphipathic helical structure. The transmembrane domain (TMD), a hydrophobic carboxy (C) terminus, anchors the protein to the membrane (Figure 1). The MSP domain is known to interact with FFAT (two phenylalanine in an acidic tract) motif containing proteins (Loewen et al., 2003) such as the oxysterol-binding protein (OSBP or ORP) family of proteins (Wyles et al., 2002), ceramide transport protein (Kawano et al., 2006) and NIR phospholipid transfer proteins (Lev, 2004). This interaction results in

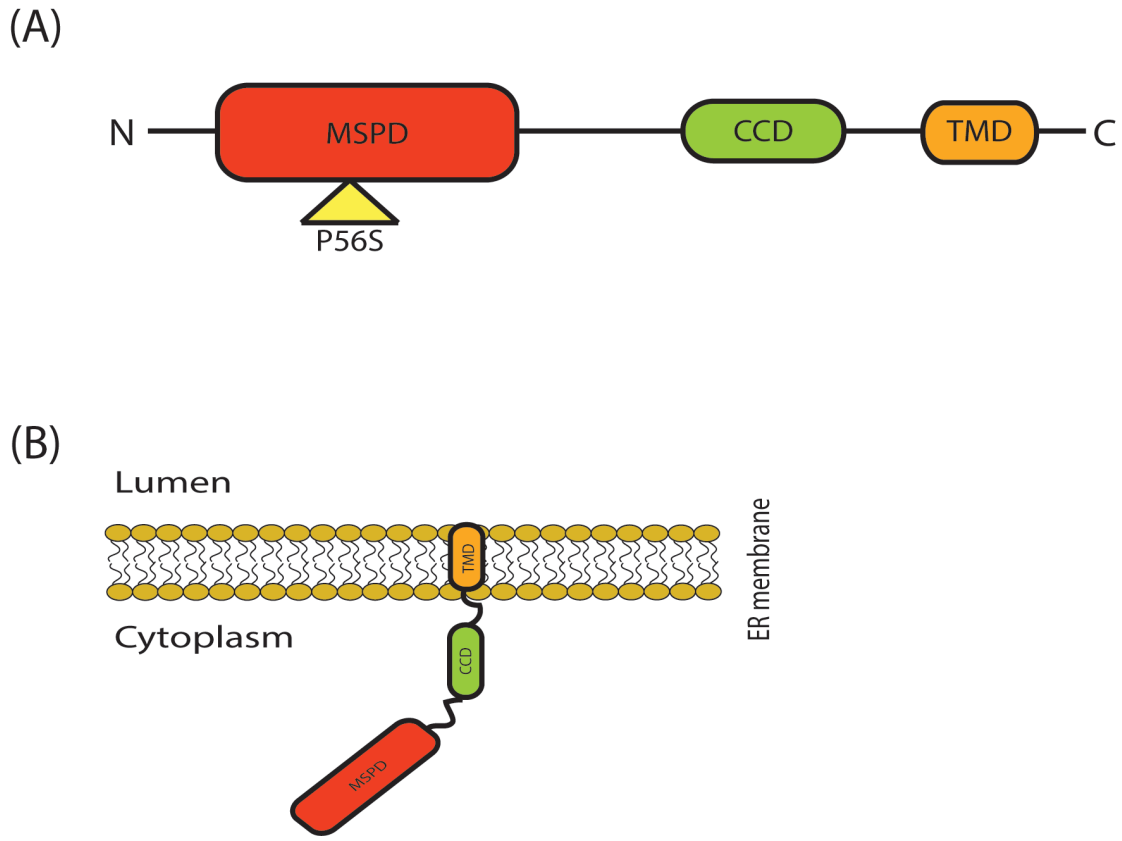

Figure 1. Schematic of VAPB protein structure.

(A) Schematic of VAPB isoforms showing the major structural domains. VAPB contains an N-terminal major sperm protein (MSP) domain, a middle coiled-coil domain (CCD), and a C- terminal transmembrane domain (TMD). 'P56S' indicates the site of the missense mutation associated with ALS8 in VAPB (VAPB-P56S).
(B) Diagram of VAP protein structure orientation. VAPB is a type II integral membrane protein. Its TMD is anchored to the ER membrane and the MSP domain is oriented towards the cytosol.

coordinated membrane recruitment by VAPs and has been shown to affect organelle morphology through regulation of lipid composition at membrane contact sites (Levine and Munro, 2001; Loewen et al., 2003).

The proline to serine substitution at the 56th codon of VAPB is housed in the MSP domain. The normal crystal structure of the MSP domain reveals that it forms a seven-strand immunoglobulin-like β sheet sandwich, where the proline at the 56th residue forms a cis-peptide bond conformation crucial in preserving the S-shaped loop (Figure 2). However, the P56S mutation that causes the proline to be substituted for serine switches the hydrogen-bonding pattern between the β sheets, which removes a kink between two short stretches of β strands, causing destabilization, misfolding and insolubility of the MSP domain (Suzuki et al., 2009). The change in the structure exposes a hydrophobic patch (Furuita et al., 2010; Kim et al., 2010), which causes the protein to be increasingly prone to the accumulation of large ER dilations in cells (Kanekura et al., 2006) (Figure 2).

Cellular consequences of VAPB-P56S

The expression of VAPB-P56S results in two main structural changes in the cell. It leads to the loss of the characteristic reticular tubular pattern of the ER and consequential ER defect (Prosser et al., 2008) as well as a loss of integrity of the nuclear envelope (Tran et al., 2012).

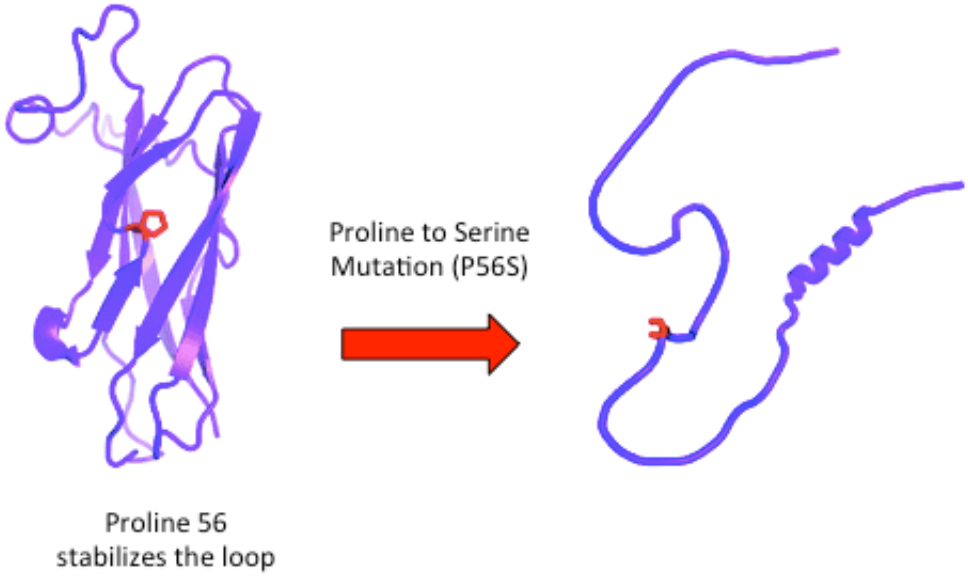

Figure 2. Structure of VAPB-WT and VAPB-P56S MSP domain.

Determination of the crystal structure reveals that the seven-stranded immunoglobulin-like β sandwich of the WT, in which Pro56 creates a cis-peptide bond conformation that stabilizes the S-shaped loop, unfolds and loses its tightly packed secondary structure as a result of a proline to serine substitution at the 56th residue. This structural change exposes hydrophobic residues.
(Figure adapted from Shi et al. (2010). Biochemistry)

VAPB-P56S causes an ER defect

The ER is an important organelle where proteins such as secretory and membrane proteins are synthesized and folded by ER chaperones. However, genetic or environmental factors, including oxidative stress, can disrupt ER homeostasis and lead to an accumulation of unfolded or misfolded proteins in the ER lumen, which is a condition called ER stress (Xu et al., 2005). This stress activates the Unfolded Protein Response (UPR), a signaling pathway that responds to alleviate and reestablish normal ER function (Ron and Walter, 2007). The accumulation of unfolded or misfolded proteins in the ER is toxic so if ER stress cannot be alleviated, cell death can be induced (Kim et al., 2008).

Aberrant misfolded protein accumulation and consequential ER stress represent a pathological hallmark of ALS. Previous studies have shown that VAPB is physiologically involved in mediating UPR since the knockdown of endogenous VAPB expression with small interfering RNA (siVAPB) attenuates UPR to DTT-induced ER stress (Kanekura et al., 2006). Also, the overexpression of VAPB-WT promotes UPR. However, the P56S mutation in a single allele abolishes the ability for VAPB to facilitate UPR to half its normal level (Kanekura et al., 2006), which could lead to sustained ER stress.

VAPB is integrated to the ER, which is involved in diverse cellular processes such as an entry point for lipid biosynthesis and secretory and membrane proteins. Its characteristic reticular pattern is dependent on its association with the microtubule network and stable anchor points provided by motor and non-motor proteins. Whereas motor proteins such as kinesin provide the mechanical force needed for ER extension along the microtubules, non-motor proteins such as VAPB provide stability by anchoring the ER membranes to microtubules. Subsequently, disrupting these anchor points will

cause a collapse in peripheral ER tubules (Andrade et al., 2004).

The mutant VAPB is highly aggregate-prone due to the structural change in the MSP domain that exposes hydrophobic residues (Teuling et al., 2007). Through cell-culture experiments analyzing the subcellular localization of wild-type (VAPB-WT) and VAPB-P56S, the over-expression of VAPB-P56S appears to cause an accumulation of membranous aggregates as well as a reduction in the characteristic reticular pattern of the ER (Figure 3) (Prosser et al., 2008). Calreticulin, a protein localized to the ER, is retained in the large membranous aggregates, which strongly suggests that the ER is the origin of these stable aggregates (Prosser et al., 2008). Further, the VAPB-P56S mutation acts in a dominant negative fashion as its central coiled-coil domain in the cytosolic tail and the TMD is able to dimerize and recruit endogenous, wild-type VAPB into its insoluble mutant clusters (Teuling et al., 2007), effectively reducing cellular levels of endogenous VAPB. The formation of dilated ER membranes induced by VAPB-P56S is suggested to compromise intracellular membrane transport and secretion. This may then cause a loss of extracellular trophic signals or a disruption of intracellular processes (Nishimura et al., 2004b), such as the blockage of ER-to-Golgi transport of proteins, thereby contributing to ER stress-induced neuronal death (Prosser et al., 2008).

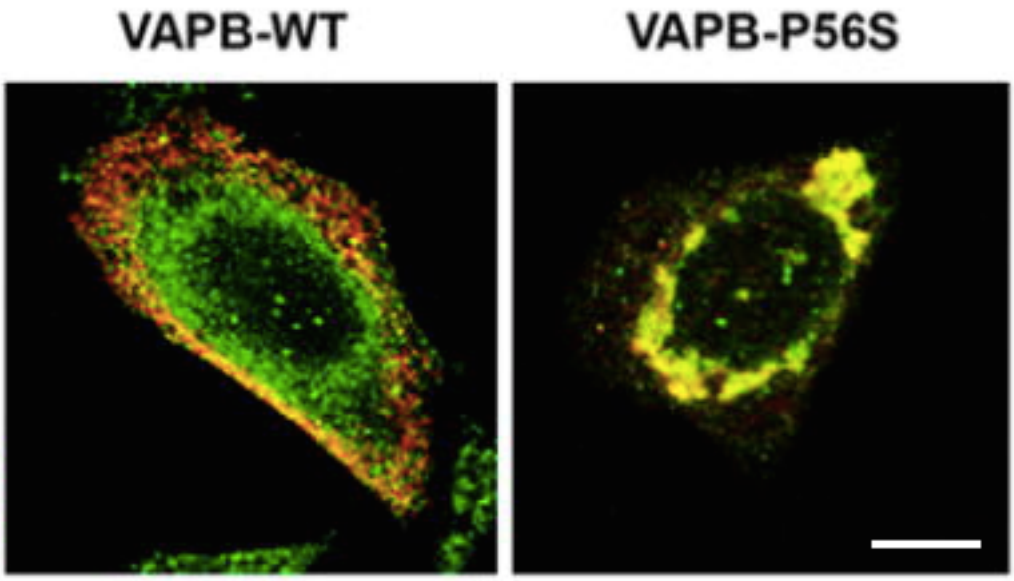

Figure 3. Subcellular localization of VAPB-WT and VAPB-P56S.

Chinese hamster ovary (CHO) cells were transfected with FLAG-tagged VAPB-WT and FLAG-tagged VAPB-P56S. FLAG-tagged VAPB-WT (red) co-localizes with ER marker, Calreticulin (green). VAPB-P56S (red) aggregates around the nucleus and there is a loss of reticular ER structure. Scale bar = 10 μm.
(Figure obtained from Prosser et al. (2008) Journal of Cell Science)

VAPB-P56S also causes a nuclear envelope defect

There is continuity between the lumen of the nuclear envelope and the rough endoplasmic reticulum (rER) as the outer nuclear membrane is continuous with the membrane of the rER, and it is also studded with ribosomes. Both these regions are responsible for protein synthesis, and secretory proteins are translocated to the ER lumen at these sites. VAPB is localized in the ER, more specifically, in the ribosome-rich areas of the rough ER, as well as in the pre-Golgi intermediates (ERGIC) (Kuijpers et al., 2013). Through cell culture studies, it was found that expression of VAPB-P56S caused a separation of the inner and outer nuclear envelope membranes, shown by the 'herniated' nuclear envelope in Figure 4 (Tran et al., 2012). Additional analyses showed that the mutation also blocked the transit of nucleoporins and nuclear membrane proteins, such as gp-210 and emerin, to the nuclear envelope, and sequestered them in the ER dilations. This mislocalization induced by the aggregate-prone VAPB-P56S may be causing the nuclear envelope defect, as nuclear pores spanning the two nuclear membranes contribute to the normally close apposition of the membranes. Furthermore, the defect appeared to be a result of the loss of function of VAPB as knocking down VAPB using siRNA produced the same effect on the nuclear envelope. This suggests that VAPB is required for entry of nuclear envelope proteins to the nuclear envelope (Tran et al., 2012).

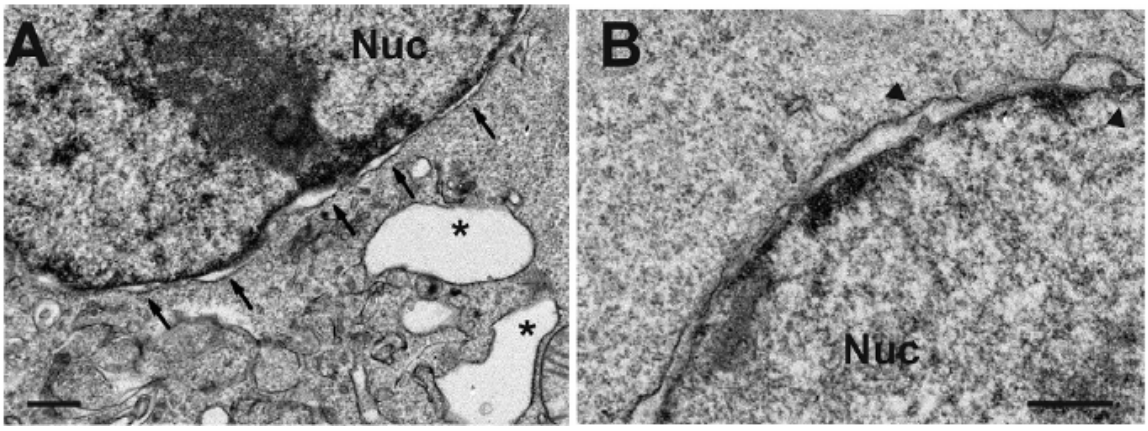

Figure 4. Overexpression of VAPB-P56S causes a nuclear envelope defect.

An electron micrograph of CHO cells transfected with VAPB-P56S shows (A) large, vacuole-like membrane structures (*) as well as a swelling of the nuclear envelope (arrow). (B) shows a magnified image of the nuclear envelope defect with membrane vesicles in the perinuclear space (arrowhead). Scale bar = 500 nm
(Figure obtained from Tran et al. (2012) Journal of Cell Science)

Decreased VAPB expression in sALS and fALS

VAPB is ubiquitously expressed and widely distributed across all tissues and throughout the central nervous system (CNS). In all areas of the brain, VAPB immunoreactivity was largely found in neuronal cell bodies and dendrites with little labeling present in glia (Teuling et al., 2007). The motor neurons of the spinal cord and caudal brainstem exhibit the highest levels of VAPB (Teuling et al., 2007). However, in a study that examined the spinal cord of 39 ALS patients (35 sALS and 4 fALS), the expression of VAPB mRNA was significantly reduced by 22%. Upon comparing the levels of VAPB from samples of those who had a long progression of disease versus a rapid one, patients that died between 1-3 years after diagnosis had a significant decrease in VAPB levels compared to the control, whereas this was not the case in ALS patients with a longer progression between 4-20 years (Anagnostou et al., 2010). Furthermore, motor neurons derived from induced pluripotent stem cells (iPSC) of ALS8 patients showed reduced protein levels of VAPB as well as a lack of cytoplasmic aggregations characteristic of previous studies overexpressing VAPB-P56S (Mitne-Neto et al., 2011). Together, this gives rise to the notion that pathogenesis is due to a loss of VAPB function.

Current ALS8 Animal Models

In addition to discoveries illustrating features of ALS8 from *in vitro* studies, *in vivo* models for the disease have also been created. Animals are often used in experimental investigations such as studying human disease due to their unlimited supply and ease of manipulation. With their similarity to human anatomy, genetics and

physiology, animals can be induced with human diseases and subsequent analyses can be performed to gain insights on the characteristics of a particular disease. Presently, there are mouse, *Drosophila melanogaster*, and *Danio rerio* models of ALS8.

Drosophila models

Two recent *Drosophila* models were created for ALS8. In 2002, a transgenic mutant VAPB fly model, ablating the *Drosophila* ortholog, DVAP-33A, was created (Pennetta et al., 2002). In 2008, a fly model using the corresponding mutation in DVAP-33A (P58S) was generated (Ratnaparkhi et al., 2008). The subsequent studies reconfirmed two key points: the VAPB-P56S mutation acts in a dominant negative fashion and VAPB-P56S may have little to no residual function.

Flies with a loss of DVAP-33A displayed motor defects including a severe decrease in the number of boutons in the muscles of the abdominal segment and a consequent increase in bouton size. The overexpression of DVAP-33A resulted in an increase in the number of boutons and a decrease in size. Interestingly, similar to flies with a loss of DVAP-33A, human VAPB-P56S expression in flies with wild-type DVAP-33A also caused a decrease in the bouton number and increase in their size, indicating that VAPB-P56S may be acting in a dominant negative manner. Furthermore, human VAPB-P56S expression in the fly model was only able to partially salvage the DVAP-33A null model while human VAPB-WT was able to fully rescue the phenotypes, signaling only a residual function of the mutant VAPB (Pennetta et al., 2002).

On the other hand, the ALS8 fly model generated by Ratnaparkhi and colleagues expressing the corresponding mutation in DVAP-33A (VAP-P58S) resembled phenotypes of VAP loss of function mutants and were opposite of VAP overexpression,

indicating that the P58S mutation does not have a residual function and acts in a dominant negative fashion. VAP-P58S appeared to aggregate, recruit wild type protein, and was ubiquitinated. Furthermore, the expression of the mutant protein resulted in impaired BMP signalling at the neuromuscular junction, which may indicate a possible mechanism of ALS8 pathogenesis since a loss of BMP signaling has been shown to cause defects in synaptic growth and function (Ratnaparkhi et al., 2008).

Mouse models

To date, three different groups have created mouse models for ALS8 by either overexpressing VAPB-P56S or ablating the VAPB ortholog in mice. In 2010, the overexpression mouse model created by Tudor and colleagues demonstrated that expressing VAPB-P56S in the nervous system using a prion gene promoter did not produce any overt motor phenotype, loss of motor neurons or alterations in survival. However, the mice showed cytoplasmic TDP-43 accumulations in the spinal cord motor neurons, which is a hallmark of ALS and has been detected in human sALS spinal cords (Tudor et al., 2010a).

In 2013, two separate groups created a mouse with the VAPB ortholog, vapb, ablated and another overexpression of human VAPB mouse model. The vapb -/- mice exhibited mild, late-onset motor deficits but no defects in the neuromuscular junctions or any muscle denervation. These mice demonstrated age-related central nervous system defects observed from their lower hind limb and ventral tone, mild tremors during the open-field tests, and an inability to remain on an accelerating rotarod despite no significant decrease in strength from grip tests (Kabashi et al., 2013). On the other hand, the most recent overexpression mouse model for ALS showed that ALS-related VAPB-

P56S differentially affected the function and survival of corticospinal and spinal motor neurons. The transgenic mice heterologously expressed human VAPB-WT and VAPB-P56S under a strong *Thy1.2* pan-neuronal promoter. The VAPB-P56S mice displayed progressive hyperactivities as well as other motor defects, including a deficit in motor coordination and balance as well as an early gait abnormality that did not worsen with age. Further, the mutant VAPB mice had large puncta in the soma and proximal dendrites of its corticospinal motor neurons and spinal motor neurons, along with an increase in ER stress, UPR and pro-apoptotic factors. Moreover, although there was no loss of spinal motor neurons, this overexpression mouse model was the first to show any motor neuron death with evidence of a progressive loss of corticospinal motor neurons mainly in the motor cortex (Aliaga et al., 2013).

Danio renio models

In 2013, Kabashi and colleagues produced a *Danio renio*, or zebrafish, model to investigate whether the loss of function of VAPB would be sufficient in causing motor neuron degeneration. Instead, although this model showed that knocking down VAPB caused swimming defects in larval zebrafish, only minor axonal defects in terms of outbranching and axonal length were observed. Furthermore, this zebrafish model provides additional evidence that VAPB-P56S is a loss of function mutation since expressing human mutant VAPB was unable to rescue the motor phenotype whereas human wild-type VAPB was able to (Kabashi et al., 2013).

Limitations of Current ALS8 Animal Models

Although previous ALS8 animal models exhibited different motor deficits and provided significant insight into the characterization of VAPB-P56S *in vivo* such as reconfirming its dominant negative function and loss of function mutation, the fish and fly models did not recapitulate the age-dependent neuronal loss that is typical of human ALS cases. In fact, only one of the three different mouse models showed evidence of neuronal death, albeit selective to a specific group of corticospinal neurons. Nevertheless, age-dependent onset of neuronal loss is difficult to assess due to the longevity of the mouse. While each model provides invaluable information, a *C. elegans* model for ALS8 may be a possible new model that could shed light on the role of VAPB in motor neurons, and its short lifespan may be beneficial to evaluating progressive neuronal degeneration.

Caenorhabditis elegans as a model organism

In 1965, Sydney Brenner introduced a 1.3 mm long, free-living, soil nematode as a model organism to study development, including neural development (Brenner, 1974). Today, these nematodes, *Caenorhabditis elegans (C. elegans)*, are important animal models in various areas of research including molecular biology, developmental biology, genetics, toxicology and neurobiology. Interestingly, there is a strong conservation of cellular and molecular pathways between worms and humans (Kaletta and Hengartner, 2006). However, it is not only its similarity to the human genome that makes *C. elegans* an advantageous animal to use. In addition, *C. elegans* are anatomically simple, transparent, have a short life span (Figure 5) and a 3-day reproductive cycle. They have a

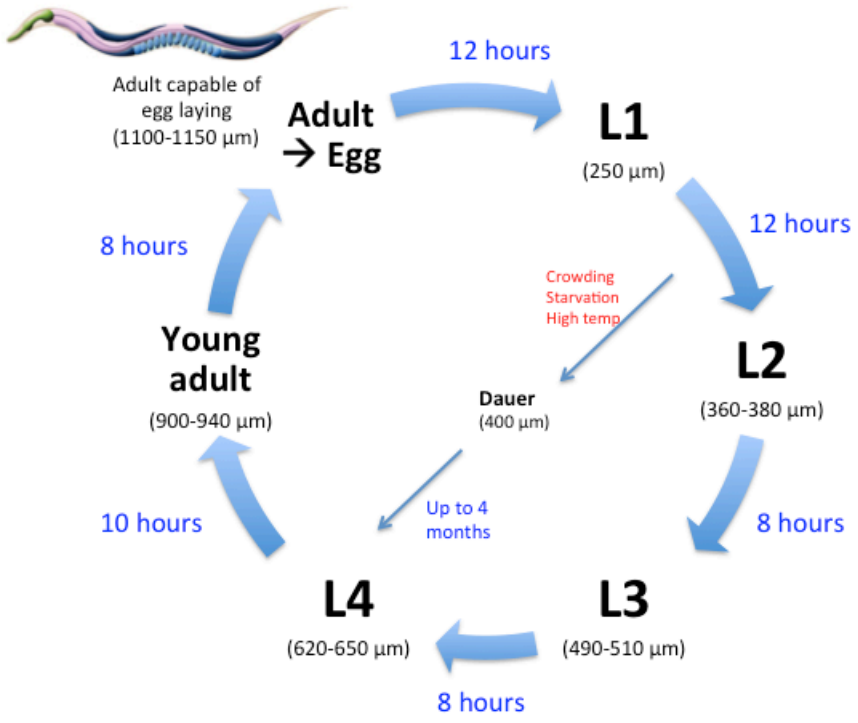

Figure 5. Lifecycle of *C. elegans* at 22°C.

Numbers next to each arrow indicate the length of time the worm spends in a certain stage. First cleavage occurs at about 40 minutes post-fertilization. Eggs are laid outside at about 150 minutes post-fertilization during the gastrula stage. The length of the worm at each stage is marked below the stage name in micrometers (µm). The dauer stage allows *C. elegans* to endure harsh environmental conditions such as crowding, starvation or high temperatures. (Adapted from Altun and Hall, 2009)

compact genome that was completely sequenced by 1998, as well as a simple and well-defined nervous system. With its observable mutant phenotypes and easy cultivation within a laboratory, *C. elegans* have developed an increased role in many fields of research.

Genetic crosses can be completed without difficulty between strains of *C. elegans* as each adult produces a large progeny (Lewis and Fleming, 1995). The two *C. elegans* sexes include a hermaphrodite (XX), which is self-fertilizing, as well as a male (XO), which arises through spontaneous non-disjunction of the hermaphrodite germ line at an infrequent 0.1% as opposed to up to 50% frequency through mating (Figure 6). Since self-fertilization gives progeny that are homozygous and genetically identical, as opposed to the movement of mutations between strains, maintenance of mutant strains and isolation made possible by mating with males, the two sexes are essential in the creation of transgenic worms through genetic crossing to produce specific genotypes (Jorgensen and Mango, 2002).

C. elegans Nervous System

The adult, hermaphrodite has 959 cells and two separate and independent nervous systems consisting of a total of 302 neurons: a large somatic nervous system (282 neurons) and a small pharyngeal nervous system (20 neurons) (Figure 7). Due to topology and synaptic connection patterns, the neurons are classified in 118 classes and because of their circuitry, the neurons can be classified by their functional properties (White et al., 1976; White et al., 1986). This leads to motor, sensory, polymodal and interneuron categories. However, because ALS is characterized by the death of upper and

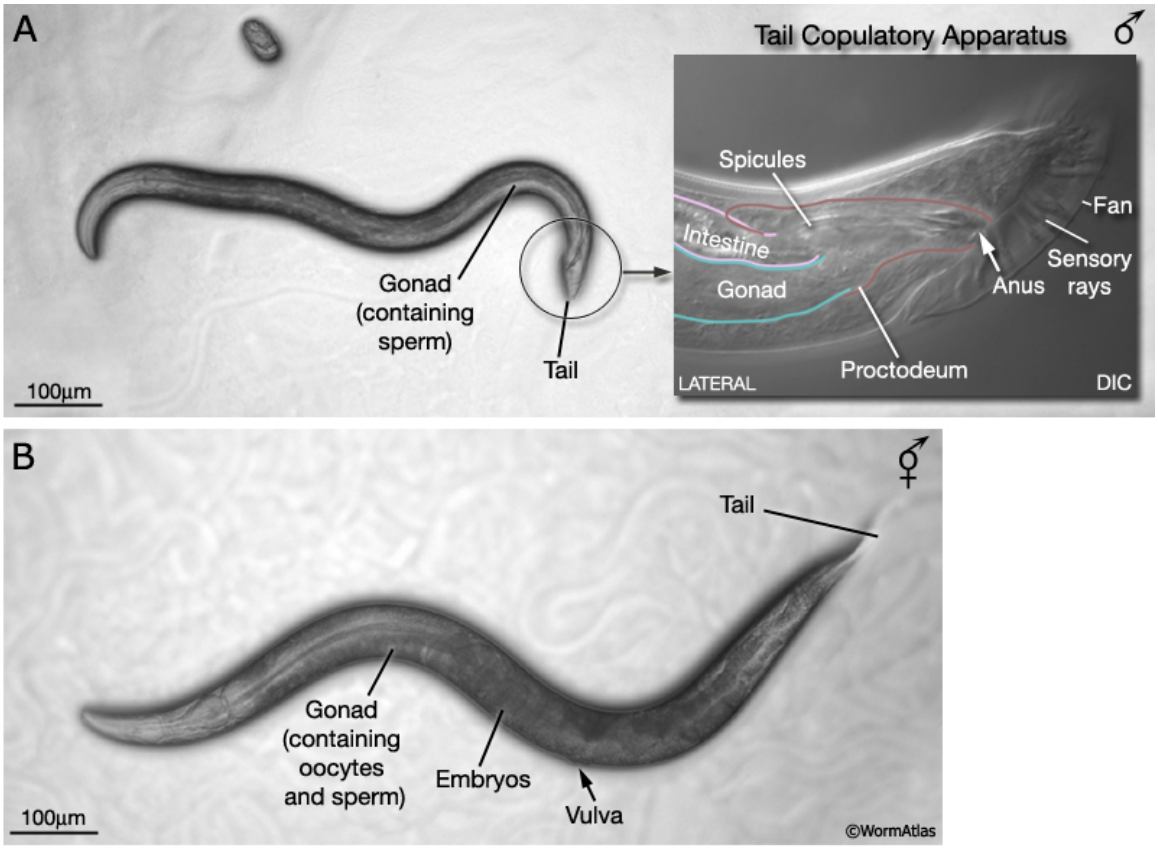

Figure 6. Light microscopy image of male (A) and hermaphrodite (B) anatomy.

Inset shows a magnified view of the tail region by Nomarski (DIC).
(Figure obtained from Wormatlas.org)

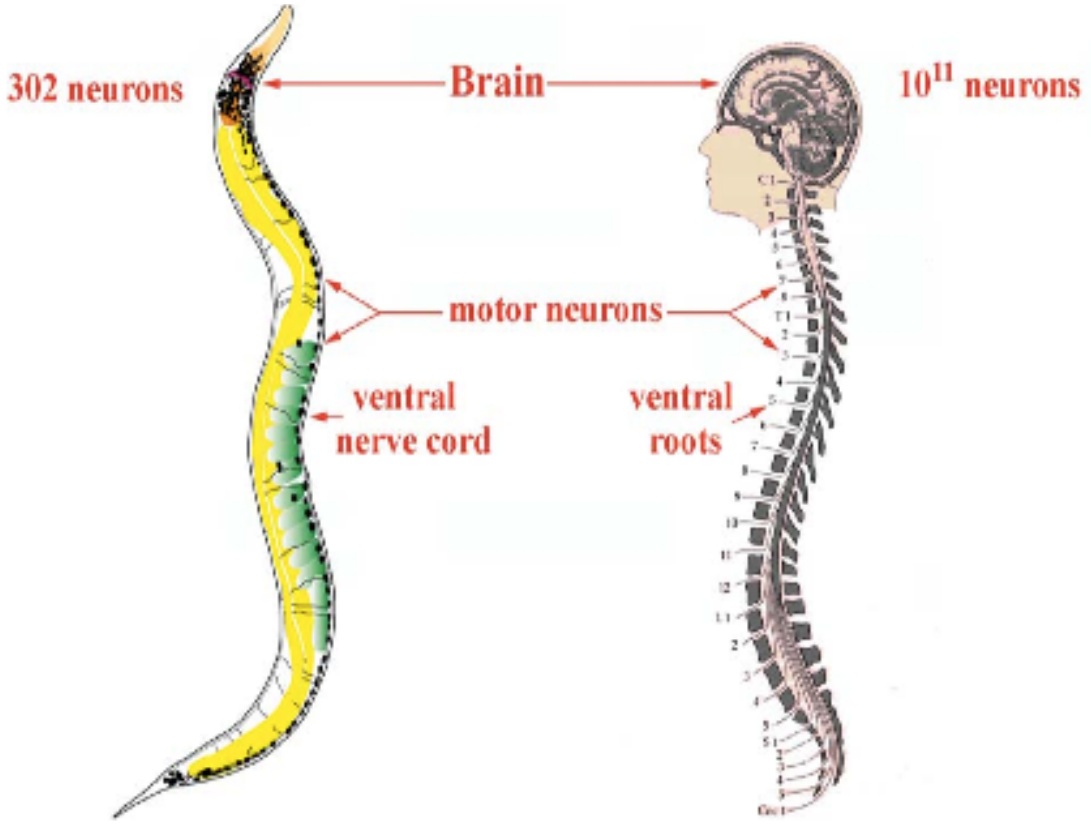

Figure 7. General comparison of the nervous systems of *C. elegans* and humans. (Figure obtained from Dr. Jonathan Hodgkin, University of Oxford.)

lower motor neurons, the motor neurons are the main focus in using *C. elegans* as a model for the disease.

C. elegans locomotion and motor neurons

Of the 302 neurons, 113 neurons are motor neurons that control locomotor behaviour such as "crawling" across solid surfaces, "thrashing/swimming" in liquid media and the motility of systems such as the reproductive and alimentary systems (White et al., 1976; White et al., 1986). Classes of motor neurons that are easily visible and often used in worm neuronal studies are the "dorsal A" (DA) and "dorsal B" (DB) cholinergic motor neurons. These are ventral cord motor neurons that innervate dorsal muscles by sending commissures to the dorsal side (White et al., 1986). The nine DA motor neurons, with commissures directed towards the anterior end, are responsible for backward locomotion. Meanwhile, the seven DB neurons, with commissures directed towards the posterior end, are responsible for forward locomotion (Figure 8) (White et al., 1976; White et al., 1986). Although *C. elegans* move in a forward sinusoidal motion, its movement is interrupted with occasional turns and reversals. Immediate reversals in locomotion can also be induced upon touch stimulus at the anterior body (Gray et al., 2005).

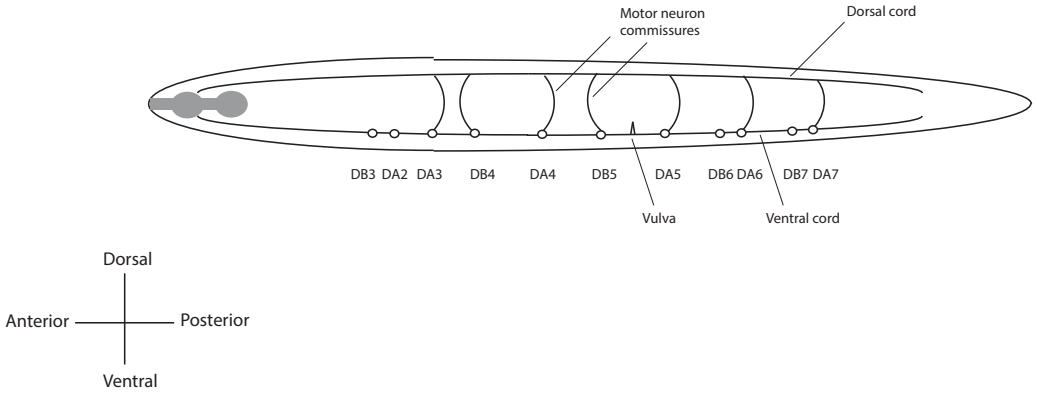

Figure 8. Adult hermaphrodite *C. elegans* "Dorsal A" (DA) and "Dorsal B" (DB) motor neurons.

Ventral cord DA and DB motor neurons innervate the dorsal muscles by sending commissures to the dorsal side. DA neurons control backward locomotion whereas DB neurons control forward locomotion. The open circles represent the cell bodies of the motor neurons and the triangle is the vulva. DA1, DB1, DB2 are not usually visible. (Adapted from Altun, Z.F. & Hall, D.H. (2011))

C. elegans RNAi Knockdown

C. elegans serve as very powerful genetic tools and continue to aid in genetic discoveries. In *C. elegans,* mutations are important tools for uncovering the function of a gene. Classical forward genetic screens are very useful in identifying genes that act in a particular process through genome-wide mutagenesis, which causes DNA lesions and mutants with a particular phenotype of interest can then be found. Subsequently, through molecular techniques and analyses, the mutated gene can be identified and its function can then be revealed. Another strategy in genetic studies involves reverse genetics, which uses RNA-mediated interference (RNAi) to knockdown a gene and establish its role.

In 1998, Fire and Mello found that double stranded RNA (dsRNA) could be injected directly into *C. elegans* to generate RNAi, and with the help of RDE-1, the Argonaute protein for *C. elegans,* a specific degradation of the endogenous target mRNA can occur (Fire et al., 1998). RNAi knockdown of a gene can also be induced by either feeding the worms with bacteria expressing the dsRNA (Timmons and Fire, 1998) or soaking the worms in a solution of it (Tabara et al., 1998). Although simply feeding dsRNA expressed by *E. coli* is not very labor-intensive, neurons are, unfortunately, resistant to RNAi feeding (Asikainen et al., 2005). However, injecting dsRNA under a specific *C. elegans* neuron promoter would allow for the neurons (cholinergic neurons in particular) to be sensitive to RNAi (Asikainen et al., 2005). This is an effective technique as the level of false positives in RNAi knockdown in worms is very low (< 1%, (Kamath et al., 2003)) and the induction of a phenotype is a reliable sign of a positive knockdown result (Kamath et al., 2003).

VPR-1

VAMP-associated protein (VAP) is phylogenetically conserved and there are orthologs across many species such as *C. elegans*. *vpr-1* encodes the *C. elegans* ortholog of VAP (Mitne-Neto et al., 2011) and is ubiquitously expressed as well. At 245 amino acids in length, VPR-1 has 56% similarity at the amino acid level with human VAPB, which is 243 amino acids long. VPR-1 is also a transmembrane protein containing a 125 amino acid N-terminal major sperm domain (MSP) with the same seven-stranded β sheet sandwich as the MSP domain of VAP (Baker et al., 2002). The MSP domain, which is conserved in many proteins of various eukaryotes, was named after its similarity to *C. elegans* MSP protein (Nishimura et al., 1999).

C. elegans MSP protein, the most abundant protein in nematode sperm (Bottino et al., 2002), does not have a transmembrane domain or coiled-coil domain, which are two of the structural domains in VAP proteins. With its intracellular cytoskeleton function and ability to polymerize without actin or myosin, MSP protein is able to facilitate the amoeboid motility of nematode sperm (Bottino et al., 2002; Tarr and Scott, 2005). It is also secreted from the cytosol of the sperm into the reproductive system to signal extracellularly during fertilization. It binds to VAB-1 Eph receptors on the oocyte to prepare it for fertilization and embryogenesis by inducing oocyte maturation and ovarian muscle contraction (Miller et al., 2001).

During embryonic and post-natal development, cells use receptor tyrosine kinases to respond to its surroundings, including growth factors and morphogens (Palmer and Klein, 2003). Receptor tyrosine kinases bind specific ligands to detect environmental changes and transmit information. Eph receptors are a group of evolutionarily conserved

tyrosine kinases that bind ephrins, which are membrane-attached ligands that inhibit oocyte maturation (Miller et al., 2003). Conversely, MSP is an antagonist to this pathway and it is believed that the MSP domain of VPR-1, as well as in *Drosophila* and mammals, is cleaved and secreted by an unconventional mechanism to perform the same function (Tsuda et al., 2008). However, the VAPB-P56S mutation in humans causing ALS8, or P58S in *Drosophila* VAP-33, resulted in mutant and wild-type protein accumulation in the ER, an unfolded protein response (UPR) that may affect cell viability, as well as an inability to secrete the MSP domain, which could influence motor neuron survival and muscle function (Tsuda et al., 2008).

vpr-1 is vital for the development of the worm and a knockout is embryonic lethal. It is required in both vab-1-dependent and independent pathways for proper distal tip cell migration during somatic gonad development as well as in ventral hypodermal cell migrations during embryonic enclosure and amphid neuron migration (Miller et al., 2001). *vpr-1(tm1411)* is a maternal-effect sterile mutant worm due to its germ cells' inability to differentiate into oocytes and sperm (Han et al., 2013). Studies have shown that the *vpr-1(tm1411)* null mutant worm had increased fat levels in adult body wall muscle, and *vpr-1* seemed to act cell non-autonomously from neurons to regulate fat accumulation in muscles. This change in fat metabolism is believed to be a compensatory mechanism facilitated by the DAF-16/FoxO transcription factor to not only elevate muscle triacylglycerol accumulation, but also increase ATP levels and prolong survival in the mutant worm (Han et al., 2013). Previous findings report ALS8 to be a disease with abnormalities in energy metabolism, which encompass various irregularities such as mitochondrial defects in the neurons and skeletal muscle, dyslipidemia, and insulin

resistance (Dupuis et al., 2011). Further, in certain ALS patient populations, a higher LDL/HDL ratio is connected to a higher survival time (Dorst et al., 2011; Dupuis et al., 2008), similar to the results from *vpr-1(tm1411)* studies. Thus, this may imply that the reduced or lack of MSP signaling from *vpr-1* is responsible for the metabolic alterations that are also seen in ALS patients and are not a secondary consequence to neurodegeneration (Han et al., 2013).

Hypothesis and Aims

Based on cellular studies and investigations involving animal models, the general consensus is that the autosomal-dominant ALS8 causing mutant VAPB-P56S is aggregate prone and dimerizes with endogenous VAPB-WT, acting in a dominant negative fashion. Thus, it is described as a loss of function mutation. Therefore, I hypothesize that the expression of human VAPB-P56S in *C. elegans* motor neurons will cause premature neuronal death. Alternatively, its expression might render the neurons more vulnerable to stress. In both cases, I anticipate the worms will develop motor deficits due to late-onset motor neuronal death. Furthermore, I hypothesize that the knockdown of the VAPB ortholog in *C. elegans*, *vpr-1,* will recapitulate the loss of protein function believed to be associated with human cases of ALS8, causing similar motor defects and age-dependent motor neuronal death.

To address these issues, two different *C. elegans* models were created: one expressing human VAPB-P56S and another with *vpr-1* knocked down. Firstly, transgenic *C. elegans* expressing human VAPB-P56S in DA motor neurons were generated to model the human disease. Since DA neurons are responsible for backward locomotion, reversal behavior assays were performed to observe any possible motor effects that the transgene might cause. By crossing the transgenic worms with *unc-129p::GFP* reporter strain, which expresses GFP in the DA and DB motor neurons that project circumferentially from the ventral cord to innervate the dorsal body muscles (Colavita et al., 1998), the DA neurons can be readily visualized. This allows the assessment of motor neuronal death of these specific neurons at various stages of the worm's adult life. In addition, VAPB-P56S has been linked to ER stress (Kanekura et al., 2006) and a nuclear envelope defect (Tran

et al., 2012), so the potential enhanced vulnerability of these neurons to oxidative stress can be tested. Secondly, since the current view of VAPB-P56S is that it is a loss of function mutation that is believed to be the underlying pathogenic mechanism for disease (Mitne-Neto et al., 2011), a knockdown model of the VAP ortholog in *C. elegans* (*vpr-1*) was created through RNAi knockdown. This circumvents embryonic lethality of the loss of *vpr-1*. The short life span of the worms allows easy assessment of age-dependent motor neuronal death upon loss of VPR-1 function through the GFP signal as described above. This second model can also be used to test drugs or other treatments that can delay the onset of neuronal death. This thesis describes the results from these investigations.

MATERIALS AND METHODS

Maintenance of C. elegans

Culturing C. elegans

C. elegans were grown at 22°C on 60 mm petri plates containing Nematode Growth Media (NGM) agar spread with a lawn of *Escherichia coli (E. coli)* strain OP50 as the food source.

C. elegans, which are 1 mm long and transparent, were visualized on stereomicroscopes, such as Leica MZ6 and Zeiss Stemi SV 11 Apo stereomicroscopes. These worms were maintained by transferring them from one petri plate to another using two different methods. Firstly, the plate can be "chunked". This "chunking" method involves using an autoclaved toothpick to cut or "chunk" a section of agar with worms on the surface from the original plate. The "chunk" is then moved to a new NGM agar plate. This method allows for a quick transfer of numerous worms from one plate to another, which is often used when moving dauer stage worms from starved plates. However, worms can also be maintained by using a worm picker to move individual worms to a new, fresh plate. A worm picker is a glass Pasteur pipette with a thin platinum wire at the end of it that allows for a single worm to be lifted at a time. This method is effective for placing a specific number of worms onto a fresh plate in order to start a population or for isolating and maintaining extrachromosomal transgenic arrays.

Zeiss Stemi SV11 Apo epifluorescence stereomicroscope was used to visualize the transgenic worms and a worm picker was used to pick worms with a specific

fluorescent phenotypic marker, which indicated that the worm contained the extrachromosomal array of interest.

The frequency of transferring depends on various factors such as the type of strain and the growth rate; the number of adults originally on the plate; the purpose of an experiment; and the amount of OP50 seeded on the plate. Generally, for maintenance purposes, the worms were transferred every couple of days when they ran out of their food source, OP50. If the plates were starved, there were countless worms in the dauer stage, which made it difficult to move individual worms. Thus, they were "chunked" first and the individual worms were then transferred with the worm picker on the following day.

Reagents

M9 Buffer

M9 buffer, an isotonic solution used in *C. elegans* culture, was used to wash and collect worms off agar petri plates. It was also used to rescue desiccated worms. It contained 22 mM KH_2PO_4, 42.3 mM Na_2HPO_4, 85.6 mM NaCl, 1 mM $MgSO_4$ in ddH_2O. The solution was sterilized by autoclaving.

Bleaching solution

Bleaching solution, alkaline hypochlorite solution, was used in a bleaching technique to synchronize worm populations and clean contaminated worm cultures. *C. elegans* are sensitive to the bleach, but the embryos are able to survive due to their protective egg shells. When cleaning contaminated worm cultures, the bleaching solution eliminates the contaminants while leaving a viable egg for a new generation of clean

worms. The bleaching solution was made up of a 1:1 ratio of 5 M NaOH and household bleach, 5% sodium hypochlorite. This solution was made on a regular basis to ensure effectiveness as bleach is photosensitive and loses its potency.

Levamisole

Levamisole (Sigma-Aldrich) is an anthelmintic drug that is a potent cholinergic agonist. It causes a hypercontracted paralysis of wild-type *C. elegans* that is usually followed by relaxation and death (Lewis et al., 1980). A solution of 30 mM levamisole in M9 buffer was effective in immobilizing the worms on agarose pads for *in vivo* microscopy.

Growth media plates

NGM agar plates

C. elegans were cultivated on 60 mm petri plates containing Nematode Growth Media (NGM) agar spread with a lawn of *Escherichia coli (E. coli)* strain OP50 as the food source (Brenner, 1974). Per litre of media, 3 g NaCl, 17 g bacto-agar and 2.5 g bacto-peptone was dissolved in 975 ml H_2O and autoclaved. Afterwards, 1 ml 1M $CaCl_2$, 1 ml 5 mg/ml cholesterol in ethanol, 1 ml 1M $MgSO_4$, and 25 ml 1M KPO_4 buffer was added to the cooled media. NGM agar media was poured aseptically into petri dishes. Once dried, OP50 was seeded and spread onto the surface of the agar.

Paraquat agar plates

Paraquat dichloride is a non-selective herbicide that is commonly used to induce oxidative stress. It produces reactive oxygen species (ROS) in both vertebrates and invertebrates such as *C. elegans* (Park et al., 2009). Paraquat was dissolved in ddH_2O to create a 1 M stock solution, and it was added to the NGM agar media just prior to pouring into petri dishes to achieve drug plates of specific concentrations (Caldicott, et al. 1994). 7.5 mM paraquat plates were used in the oxidative stress studies with the VAPB transgenic worms.

5'flurodeoxyuridine (FUDR) agar plates

5'flurodeoxyuridine (FUDR) is an antimetabolite that inhibits thymidylate synthase, which causes an imbalance of intracellular deoxyribonucleoside triphosphate (dNTP), leading to a disruption of DNA synthesis and cell death (Uchikubo et al., 2002). FUDR can be used to inhibit progeny growth by impeding cell division, reducing egg production and preventing eggs from hatching (Sutphin and Kaeberlein, 2009). FUDR was added to the NGM agar media just prior to pouring into petri dishes to achieve drug plates of specific concentrations. 120 μM FUDR plates were used in lifespan assay studies with VAPB transgenic worms.

DNA plasmid constructs

Promoters used

unc-4p drives gene expression in the A-type motor neurons, DA and VA, the six VC motor neurons that innervate the vulval muscles, and the three SAB motor neurons (Esmaeili et al., 2002; Lickteig et al., 2001; Miller et al., 1992).

hsp-16.2p is a promoter that allows for heat shock stress-induced gene activation through the essential heat-responsive locus *hsp-16.2* in *C. elegans* (Rohner et al., 2013). HSP-16.2 is one of the sixteen small heat shock proteins (sHSP) in *C. elegans*. Under physiological conditions, sHSPs are among the most highly inducible HSPs during thermal stress, and they are only expressed under these stress conditions (Leroux et al., 1997). Previous studies express *hsp-16.2* by heat shock (35°C for 2 hours, with some up to 4 hours) (Strayer et al., 2003).

VAPB transgenic strain constructs

For the generation of transgenic *C. elegans* expressing human VAPB-WT and VAPB-P56S, cDNAs containing FLAG-tagged human VAPB-WT and VAPB-P56S were PCR amplified from FLAG-tagged human VAPB-WT and FLAG-tagged human VAPB-P56S constructs described previously in (Prosser et al., 2008), where VAPB was subcloned into pFlag-CMV2 at the *NotI* and *BamHI* sites and the P56S mutation was generated by site-directed mutagenesis, and subcloned into pFlag-CMV2 at the *NotI* and *EcoRI* sites (Prosser et al., 2008).

To generate the expression plasmid for the transgenic VAPB *C. elegans*, the cDNAs encoding FLAG-tagged human VAPB-WT and VAPB-P56S were subcloned into

a pAC56 plasmid under the *unc-4* promoter (*unc-4p*) at the *XbaI* and *KpnI* sites. The clones were confirmed through DNA sequencing at the StemCore Laboratories at Sprott Center for Stem Cell Research, Ottawa Hospital Research Institute. The uncut, empty pAC56 plasmid acted as the DNA plasmid for creating the control strain for which strains with the expression plasmids containing human VAPB-WT and VAPB-P56S were compared against.

vpr-1(RNAi) knockdown strain constructs

For the generation of *vpr-1* knockdown *C. elegans* strains, *vpr-1(RNAi)*, the following recombinant plasmids were created. cDNA of *rde-1* was PCR amplified and subcloned into a pAC56 plasmid under the *unc-4* promoter (*unc-4p*) at the *BamHI* and *KpnI* sites. In addition, cDNA of *vpr-1* was PCR amplified, and *vpr-1 sense* and *vpr-1 antisense* were subcloned into separate pPD49_78 plasmids under the *hsp-16.2* promoter (heat shock promoter) at the *BamHI* site. An empty pAC56 plasmid was used to create the control strain used in the knockdown experiments. The pAC56 plasmid was a generous gift from Dr. Antonio Colavita (University of Ottawa, Ottawa, ON, Canada). The pPD49_78 plasmid was obtained from Addgene (Dr. Andrew Fire, Stanford University).

Strains

Heritable extrachromosomal DNA transformation was first described by Stinchcomb *et al.* in 1985 and this method was employed in generating the VAPB transgenic worms and *vpr-1* knockdown worms used in these studies. A microinjection is a simple technique of introducing exogenous DNA into *C. elegans* by injecting the DNA solution into the central core of cytoplasm in the distal arm of the gonad, which is shared by many germ cells nuclei (Mello et al., 1991). Driven by homologous recombination, at appropriate concentrations, injected DNA concatemerize into large extrachromosomal arrays. These large extrachromosomal arrays can incorporate various copy numbers, and the progeny of the self-fertilizing transformed worms inherit the DNA of the array in non-Mendelian segregation patterns. A phenotypic marker like *odr-1p::DsRed* and *myo-2p::DsRed* was co-injected to select for the transgenic worms. Microinjections were performed by David Carr and Dr. Antonio Colavita (University of Ottawa, Ottawa, ON, Canada).

Generation of VAPB transgenic strains

Transgenic VAPB *C. elegans* (VAPB-WT, VAPB-P56S, empty vector control) were generated through microinjection of DNA solutions containing the specific construct (*unc-4p::VAPB-WT, unc-4p::VAPB-P56S,* or empty pAC56 vector) along with a phenotypic marker, *odr-1p::DsRed,* using an Eppendorf Femtojet™ into N2 worms as described in Wormbook (Evans, 2005). The resulting worms were crossed with a *unc-129p::GFP* reporter strain (as described in Fay, 2006) in order to visualize the DA and DB motor neurons.

Generation of vpr-1(RNAi) knockdown strains

Because *C. elegans* neurons are resistant to RNAi knockdown via feeding (Timmons and Fire, 1998), genetic interference can be induced by microinjecting corresponding neuron-specific DNA constructs targeting a specific gene (Asikainen et al., 2005). Two plasmids were used to control 'when' and 'where' *vpr-1* knockdown occurred. Since knocking out *vpr-1* is embryonic lethal, plasmid pPD49_78 with *hsp-16.2p* (heat shock promoter) was used to induce RNAi knockdown of *vpr-1* at specific stages. pAC56 with *unc-4p* was used to control where the knockdown occurred, which was in the DA neurons specifically.

Firstly, before injecting the corresponding plasmids, *rde-1(ne219)* was crossed with *unc-129p::GFP* and a line with homozygous *rde-1(ne219)* and homozygous *unc-129p::GFP* was selected through confirmation by genomic sequencing at the Plateforme de Séquençage et de Génotypage des génomes at the University of Laval.

RDE-1 is a conserved protein of the Argonaute family of proteins required for RNA mediated interference (RNAi). In order to specifically target the DA motor neurons for *vpr-1* knockdown, *rde-1(ne219),* a *rde-1* mutant *C. elegans* lacking the essential protein in the Argonaute family for RNAi was used. In the *vpr-1(RNAi)* knockdown strain that was generated, RDE-1 function was restored only in the DA neurons by expressing *rde-1* under the *unc-4* promoter in pAC56 plasmid. As a result, only DA motor neurons expressed RDE-1 needed to mediate RNAi knockdown of *vpr-1* upon heat shock (Figure 9). The control strain was injected with an empty pAC56 plasmid so *rde-1* was not restored in the DA neurons. Consequently, despite the presence of both *vpr-1 sense* and *vpr-1 antisense* following heat shock, RDE-1 was not present to induce RNAi

knockdown of *vpr-1* in the control worms.

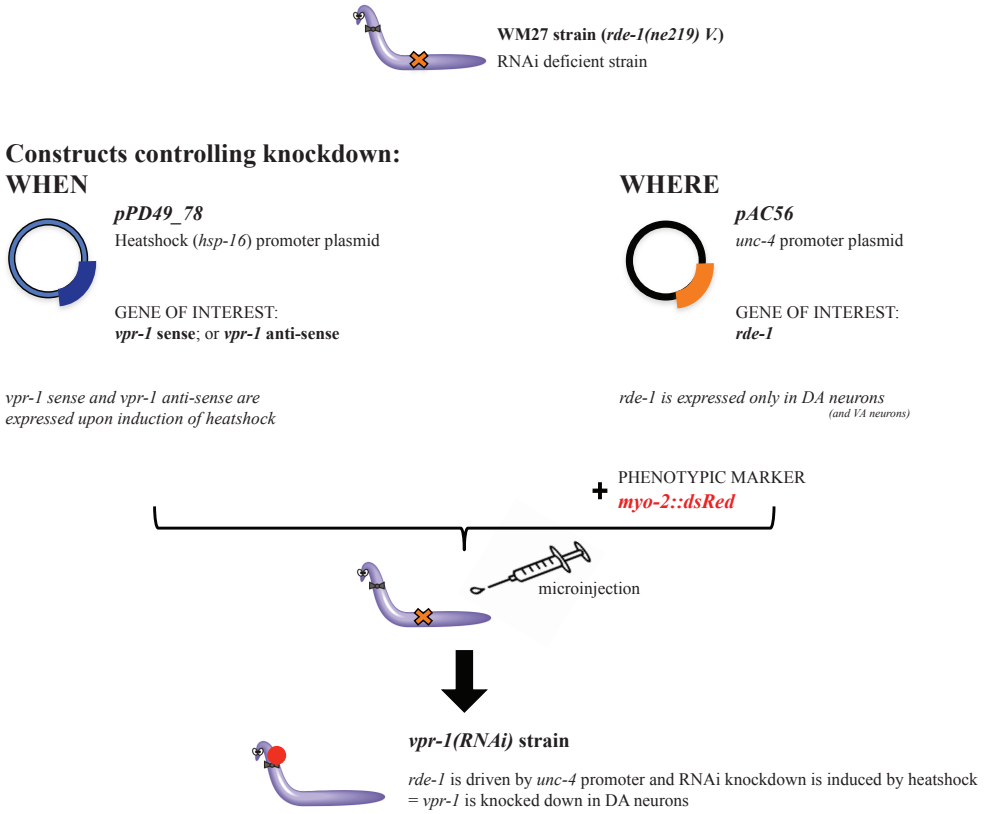

Figure 9. Schematic of the general methodology for creating the *vpr-1(RNAi)* strain.

This strain enabled the knockdown of *vpr-1* in the DA neurons. For the control strain, the same constructs were used but the pAC56 vector is empty and does not contain the *rde-1* gene.

Strains used

Table 2. *C. elegans* strains created for various experiments.

All strains were crossed with an *unc-129p::GFP* reporter strain to allow visualization of DA and DB motor neurons. Each strain used either a *myo-2p::DsRed* or *odr-1p::DsRed* as the phenotypic marker. The DNA concentrations are indicated as approximated from the concentration in the injection mix (ng/µl).

Experiment	Strain	Genotype
Background strains for injections	N2	N2
	GFP Reporter Strain	*unc-129p::GFP*
	wm27	*rde-1(ne219)*
VAPB transgenic models	VAPB-WT	*unc-129p::GFP ex[unc-4p::VAPB-WT 40 ng/µl; odr-1p::DsRed 40 ng/µl]*
	VAPB-P56S	*unc-129p::GFP ex[unc-4p::VAPB-P56S 40 ng/µl; odr-1p::DsRed 40 ng/µl]*
	Control (empty vector)	*unc-129p::GFP ex[unc-4p 40 ng/µl; odr-1p::DsRed 40ng/µl]*
***vpr-1* knockdown model**	vpr-1(RNAi)	*rde-1(ne219) unc-129p::GFP ex[unc-4p::rde-1 40ng/µl; hsp-16.2p::vpr-1 50 ng/µl; hsp-16.2p::vpr-1-as 50 ng/µl; myo-2p::DsRed 5 ng/µl]*
	Control knockdown	*rde-1(ne219) unc-129p::GFP ex[unc-4p 40ng/µl; hsp-16.2p::vpr-1 50 ng/µl; hsp-16.2p::vpr-1-as 50 ng/µl; myo-2p::DsRed 5 ng/µl]*

Microscopy

Brightfield light microscopy

For general maintenance of the *C. elegans* cultures, a stereomicroscope, such as Zeiss Stemi SV 11 Apo epifluorescence stereomicroscope or Leica MZ6 stereomicroscope, was used to visualize and transfer individual worms to new plates with the worm picker. In addition, Zeiss Stereo Discovery.V20 Microscope was used to capture brightfield images and occasionally for regular worm cultivation as well. Images were taken with the 1x objective at magnifications of 7.5x to 100x.

Fluorescence microscopy

Zeiss AxioImager.M2 epifluorescence microscope was used for all fluorescence microscopy, allowing for the visualization of individual neurons and for capturing images. 3% agarose pads were made on glass microscope slides used to mount worms with 7 µl of 30 mM levamisole. A glass coverslip was placed on top of the worms to secure them to the agarose pad for imaging. Images were taken with 10x and 20x objectives using the Zeiss AxioVision software version 4.8. Stacks of DA and DB neuron images with an interval of 0.5 µm between each slice were collapsed into a single image and processed with Image J (NIH, Bethesda, MD, USA).

Experiments

Lifespan Assay

The transgenic strain worms were maintained at 22°C on 60 mm petri plates containing Nematode Growth Media (NGM) agar spread with a lawn of *Escherichia coli (E. coli)* strain OP50 as the food source. However, for the lifespan assay, at the L4 stage, the transgenic worms (VAPB-WT, VAPB-P56S or empty vector control) were separated from the rest of the population by transferring them to a new NGM agar plate. The following day, the resulting Day 1 adulthood transgenic worms were transferred to 120 μM FUDR agar plates. Each day, the same adult transgenic worms were transferred to fresh 120 μM FUDR agar plates and maintained on these plates for 5 days before transferring them back to regular NGM agar plates until the end of its lifespan. Each day, the number of worms that were alive was recorded. Because FUDR is an antimetabolite that inhibits DNA synthesis, the embryos laid by the adult worms did not hatch, which allowed for examination of the original adult transgenic worms throughout their lifespan without any risk of mixing up the worms with new, developing worms. Survival curves were produced and compared using the Log-rank (Mantel-Cox) test.

Locomotor Behaviour Assay

Behaviour reflects the activity of the nervous system and is influenced by neuronal function. “Reversal behaviour” describes the tendency for *C. elegans* to change from forward to backward locomotion due to a modification in the direction of propagation of the sinusoidal body bends. An immediate reversal can be induced through an acute stimulus such as a harsh touch. A harsh touch to the body of the worm can be

defined by prodding it with the thin platinum wire of a worm picker just behind the pharynx. In the adult worm, this initiates immediate backward locomotion 90-95% of the time (Hart, 2006). Human observation was used to count the number of backward bends before the worm resumed forward locomotion under a Leica MZ6 stereomicroscope, and a stopwatch was used to record the length of time. One full body bend was defined as when the part of the worm just behind the pharynx reached a maximum bend in the opposite direction from the bend that was last counted. Since *C. elegans* have a distinct sinusoidal motion, one full "body turn" can also be defined as a half wavelength for a sine wave (π) (Figure 10). Worms that coiled up or only made partial body movements were deemed "uncoordinated".

The reversal behavior of Day 3 and 11 adult VAPB transgenic worms of each condition (empty pAC56 control, VAPB-WT and VAPB-P56S) was scored on unseeded NGM plates at 22°C under a Leica MZ6 stereomicroscope. Using the Zeiss Stemi SV 11 Apo epifluorescence stereomicroscope, transgenic worms were selected for the phenotypic marker, *odr-1p::DsRed* signal at its head, as containing the expression vector and gene of interest. Day 3 and Day 6 adult *vpr-1(RNAi)* worms were scored for reversal behavior under the same experimental conditions as the VAPB transgenic worms. Each trial was repeated twice with over 2 minutes between trials for each worm in all locomotor behavior experiments.

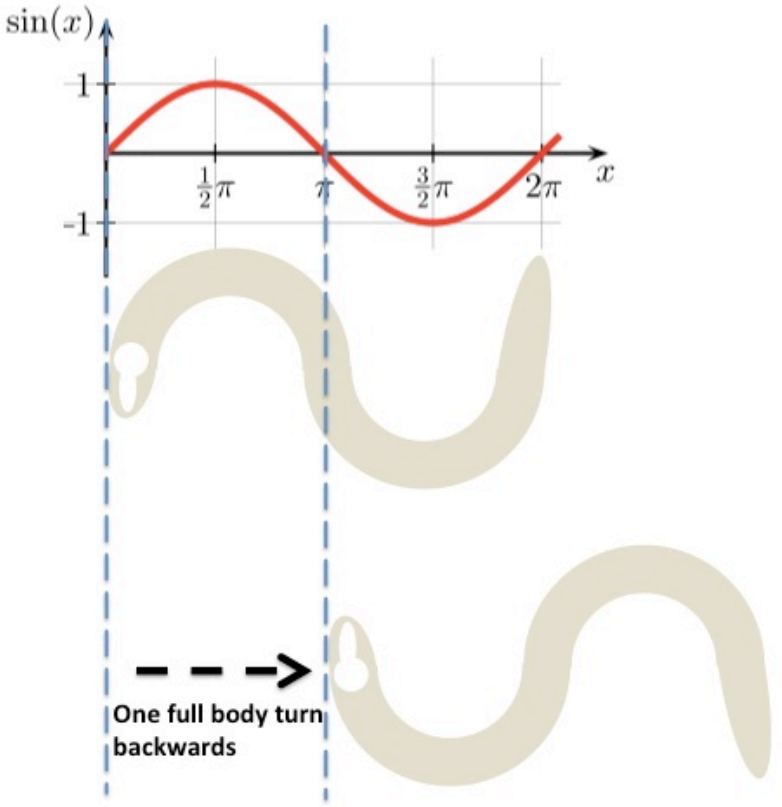

Figure 10. Schematic of the reversal behavior of *C. elegans.*

One full body bend was defined as when the part of the worm just behind the pharynx reached a maximum bend in the opposite direction from the bend that was last counted. Since *C. elegans* have a distinct sinusoidal motion, one full "body turn" can also be defined as a half wavelength for a sine wave ($\boldsymbol{\pi}$).
(The sine plot portion of the figure was obtained from betterexplained.com)

Paraquat Treatment Protocol

VAPB transgenic *C. elegans* strains treated with the oxidative stress-inducing herbicide, Paraquat, were transferred at Day 1 of adulthood to 7.5 mM Paraquat agar plates. After treating the worms for 17 hours on the Paraquat plates, the transgenic worms were transferred to untreated NGM agar plates. The worms were maintained at 22°C (unless otherwise stated) and the neurons were scored at Day 3, 7 or 11 of adulthood.

Heat shock Knockdown Protocol

Adult *vpr-1* knockdown model (*vpr-1(RNAi)* or control) worms were bleached in order to harvest the eggs, and 21.5 hours later, the larvae were heat shocked at 35°C for 2.5 hours. The heat shock was repeated at stages L4, adult Day 2, adult Day 3, and adult Day 5. The detailed heat shock times are noted in Table 3.

Table 3. Heat shock protocol for the *vpr-1(RNAi)* knockdown model.

Each heat shock was for 2.5 hours in an incubator at 35°C.
For example, the worms are bleached at 11:30 am on Monday. The following day, Tuesday, the resulting L2 worms are heat shocked at 9:00 am for 2.5 hours at 35°C.

Experiment Day	Procedure	Time	Approximate life stage	Example
0	Bleach	0 hour	Embryo	11:30 am
1	HEAT SHOCK	21.5 hours after Experiment Day 0	L2	9:00 am
2	HEAT SHOCK	25.5 hours after Experiment Day 1	L4	10:30 am
3	Select for phenotypic marker	Anytime during Experiment Day 3	Adult Day 1	Anytime during the day
4	HEAT SHOCK	47 hours after Experiment Day 2	Adult Day 2	9:30 am
5	HEAT SHOCK	23 hours after Experiment Day 4	Adult Day 3	8:30 am
6	Transfer worms	Anytime during Experiment Day 6	Adult Day 4	Anytime during the day
7	HEAT SHOCK	49.5 hours after Experiment Day 5	Adult Day 5	9:30 am
8	Image worms	Anytime during Experiment Day 8	Adult Day 6	Anytime during the day

Neuronal Misguidance or Loss Assay

The adult VAPB transgenic *C. elegans* were selected for the *odr-1p::DsRed* phenotypic marker, which was co-injected with the plasmids containing the genes of interest. 7 µl of 30 mM levamisole (Sigma) in M9 solution was applied to each 3% square agarose pad on the microscope slide before mounting the worms. Once the worms were applied to the levamisole on the agarose pad of the microscope slide, a glass coverslip was placed overtop to secure the worms. Usually, approximately 20 transgenic worms were applied per agarose pad.

The *vpr-1(RNAi)* worms were selected for their phenotypic marker, *myo-2p::DsRed,* and the microscope slides were prepared in the same fashion as the VAPB transgenic worms.

Since the VAPB transgenic worms and *vpr-1(RNAi)* worms were crossed with *unc-129p::GFP*, the axons and cell bodies of DA and DB neurons of the empty pAC56 control, VAPB-WT, VAPB-P56S and *vpr-1(RNAi)* were visualized under the Zeiss AxioplanII fluorescence microscope with a 20x objective. Visualizing the motor neurons under the fluorescence microscope allowed for scoring of DA or DB neuronal loss as well as any axonal misguidance, which is defined as incomplete axonal commissures projecting from the cell bodies or mistargeted, non-parallel axonal commissures.

In order to synchronize the population for imaging and quantifying at Day 3, 6, 7 or 11 of adulthood, adults worms were bleached and the worms from the surviving embryos were staged with respect to developmental stages as described (Kenyon, 1988; Riddle et al., 1997)

Statistical analyses

Statistical comparisons of the data were performed using an unpaired Student's t-test or either a One-way Anova or Two-way Anova followed by a post-hoc Bonferroni test. Survival curves were compared using the Log-rank (Mantel-Cox) test. All statistical analyses were conducted using the GraphPad Prism 5.0a. Results were deemed statistically significant when $p<0.05$.

RESULTS

VAPB Transgenic Strains

VAPB-WT and VAPB-P56S expression result in slowed rates of backward locomotion

Familial Amyotrophic Lateral Sclerosis 8 (ALS8), characterized by VAPB-P56S, is a late-onset, progressive, neurodegenerative disease that results in a deterioration of upper and lower motor neurons, which causes skeletal muscle atrophy. Consequentially, this leads to limb weakness, cramping, spasticity and fasciculations. These symptoms progress until the decline in diaphragm muscles leads to respiratory failure 2-5 years after diagnosis. Motor neuron degeneration and motor deficits go hand in hand as a loss of motor neurons or neuronal dysfunction can affect motor behavior. Previous animal models for ALS8, such as a *Drosophila* model by Chai *et al.* in 2008 expressing DVAP-P58S, corresponding to human VAPB-P56S, exhibit motor defects such as sluggishness and uncoordination (Chai et al., 2008). This suggests that expressing human VAPB-P56S in *C. elegans* might also cause locomotor deficits.

Driven by the *unc-4* promoter, VAPB-WT and VAPB-P56S were expressed in DA and VA motor neurons, which are responsible for backward locomotion. Upon inducing a harsh touch stimulus to the head, the worm changes from forward to backward locomotion through a change in the direction of propagation of the sinusoidal body bends called “reversal behaviour.” Reversal behaviour assays were conducted to measure the total number of body bends backward and the length of time it took between applying the stimulus and the subsequent return to forward locomotion.

Both Day 3 adult VAPB-WT and VAPB-P56S worms exhibited fewer body bends over a longer duration of time (0.42 ± 0.02 turns/second and 0.47 ± 0.03 turns/second, respectively), which resulted in a significant decrease ($p<0.001$) in the rate of backward locomotion compared to the control (0.71 ± 0.03 turns/second) (Figure 11). Statistical tests were conducted to compare the control versus VAPB-WT or VAPB-P56S at Day 3. The same tests were done at Day 11. The rate of backward locomotion decreased with aging, and overexpressing VAPB-WT or VAPB-P56S decreased the rate of locomotion further ($p<0.001$). Similar to the trend observed in Day 3 worms, the defect with VAPB-WT (0.04 ± 0.01 backward turns/second) was worse than VAPB-P56S worms (0.18 ± 0.02 backward turns/second) by Day 11. This suggests that expressing VAPB-WT and VAPB-P56S in DA neurons may have caused a possible locomotor defect in both the VAPB-WT and VAPB-P56S strains that worsened with age.

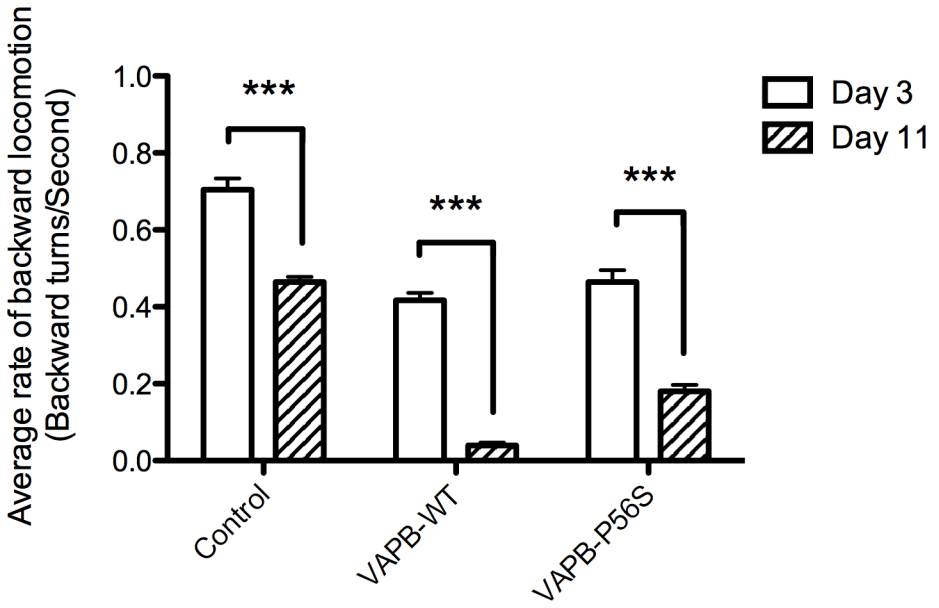

Figure 11. VAPB-WT and VAPB-P56S transgenic *C. elegans* strains exhibit a decreased rate of backward locomotion that worsens with age.

The behaviour assay was conducted by a harsh-touch method to the head of each adult *C. elegans* (Day 3 and 11 adults) directly behind the pharynx, and its initial backward movement before returning to the forward direction was recorded. Since *C. elegans* move in a distinct sinusoidal motion, one full "body turn" was defined as half a wavelength of a sine wave (π). For each VAPB transgenic strain, an average of 114 worms was quantified. The rate of backward locomotion is given as the mean rate ± S.E.M. At Day 3, the control strain made 0.71 backward turns/second ± 0.03 S.E.M. Compared to the control, VAPB-WT and VAPB-P56S strains demonstrated slower rates of 0.42 backward turns/second ± 0.02 S.E.M. ($p<0.001$) and 0.47 backward turns/second ± 0.03 S.E.M. ($p<0.001$) respectively. By Day 11, the rate of backward locomotion in the control (0.46 backward turns/second ± 0.01 S.E.M.), VAPB-WT (0.04 backward turns/second ± 0.01 S.E.M.) and VAPB-P56S (0.18 backward turns/second ± 0.02 S.E.M.) declined significantly from Day 3 (***, $p<0.001$). Statistical analyses using a One-way ANOVA followed by a post-hoc Bonferroni test was used to compare each strain with control at Day 3. The same was repeated for Day 11. Two-way ANOVA followed by a post-hoc Bonferroni test were performed to compare Day 3 and Day 11.

VAPB-WT and VAPB-P56S expression lead to axonal misguidance in "dorsal A" (DA) motor neurons

Similar to ALS cases with motor deficits, the VAPB transgenic strains expressing VAPB-P56S appeared to have a motor deficit in the form of a locomotor defect. Since locomotor behavior reflects nervous system activity, the worms were observed at the neuronal level for any defects or neuronal loss.

C. elegans are transparent throughout their life cycle, making it easy to visualize neurons under a fluorescence microscope. By crossing the transgenic worms containing the VAPB-WT, VAPB-P56S and empty pAC56 vector control with an *unc-129p::GFP* reporter strain, which expresses GFP in the "dorsal A and B" (DA and DB) motor neurons that project circumferentially from the ventral cord to innervate the dorsal body muscles (Colavita et al., 1998), the axons and cell bodies of the DA and DB motor neurons could be visualized.

Visualization of the axons projecting from the DA and DB cell bodies showed certain DA neurons with axonal misguidance, which is defined, in this case, as axon guidance defects, such as incomplete axonal commissures projecting from the cell bodies or mistargeted, non-parallel axonal commissures that fail to project directly across from the ventral cord to the dorsal side. The axons are normally parallel to each other and reach from the cell body on the ventral cord to the dorsal midline, without meandering, as observed in the control (Figure 12A). On the other hand, axonal misguidance was observed in both VAPB-WT and VAPB-P56S. For example, DA4 and DA5 neurons do not appear to innervate the dorsal side, as the commissures were misdirected laterally and fail to reach the dorsal side (Figure 12B). A similar defect was seen in DA3, DA4, DA5

and DA7 neurons of the VAPB-P56S strain (Figure 12C).

Quantification of the axonal misguidance showed that, compared to control (2.1% ± 1.2%), VAPB-WT and VAPB-P56S had significantly higher incidences of worms with one or more axons that were misguided at 96.9% ± 1.4% ($p<0.001$) and 37.2% ± 4.0% ($p<0.001$) respectively. Also, VAPB-WT worms had a significantly higher frequency of misguidance than VAPB-P56S ($p<0.001$) (Figure 13).

VAPB-WT and VAPB-P56S were expressed solely in the class A neurons and the results showed that the axonal misguidance affected DA neurons specifically, as there was little to no misguidance in DB neurons across all three strains. Various DA neurons in both VAPB-WT and VAPB-P56S strains exhibited axonal misguidance but the neurons that were most susceptible to axonal misguidance appeared to be DA6 and DA7 in VAPB-WT worms (74.8% ± 3.4%, and 67.9% ± 3.7% respectively, $p<0.001$) (Figure 14). This suggests that VAPB-WT and VAPB-P56S expression lead to neuronal dysfunction in DA motor neurons and the posterior, DA6 and DA7, motor neurons seem to be more susceptible to axonal misguidance in the VAPB-WT strain.

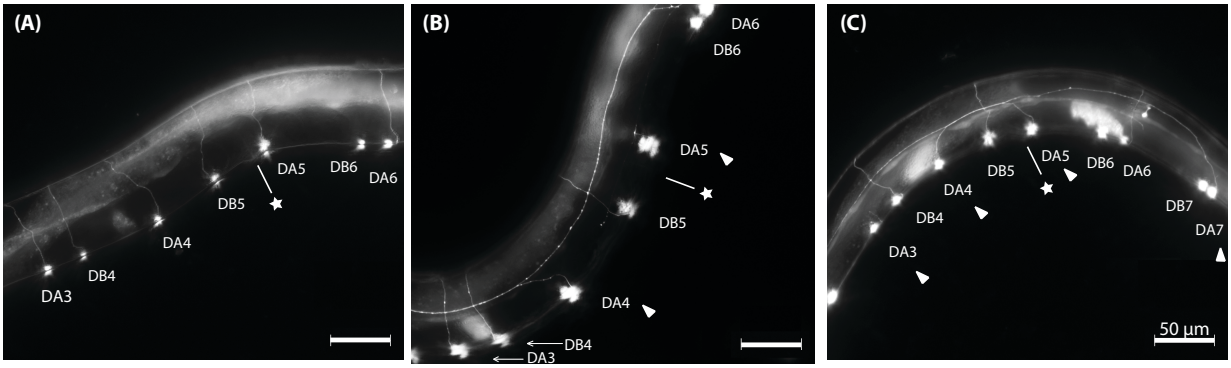

Figure 12. Dorsal A (DA) and Dorsal B (DB) neurons of transgenic *C. elegans* expressing human VAPB-WT or VAPB-P56S.

DA neurons express FLAG-tagged human VAPB-WT and FLAG-tagged human VAPB-P56S. The ventral cord DA and DB neurons innervate dorsal muscles. The transgenic worms were crossed with *unc-129p::GFP* for visualization of the axons and cell bodies of DA and DB neurons of the empty pAC56 control (A), VAPB-WT (B), and VAPB-P56S (C). Misguided axons are represented by arrowheads and the vulva is represented by a star symbol.

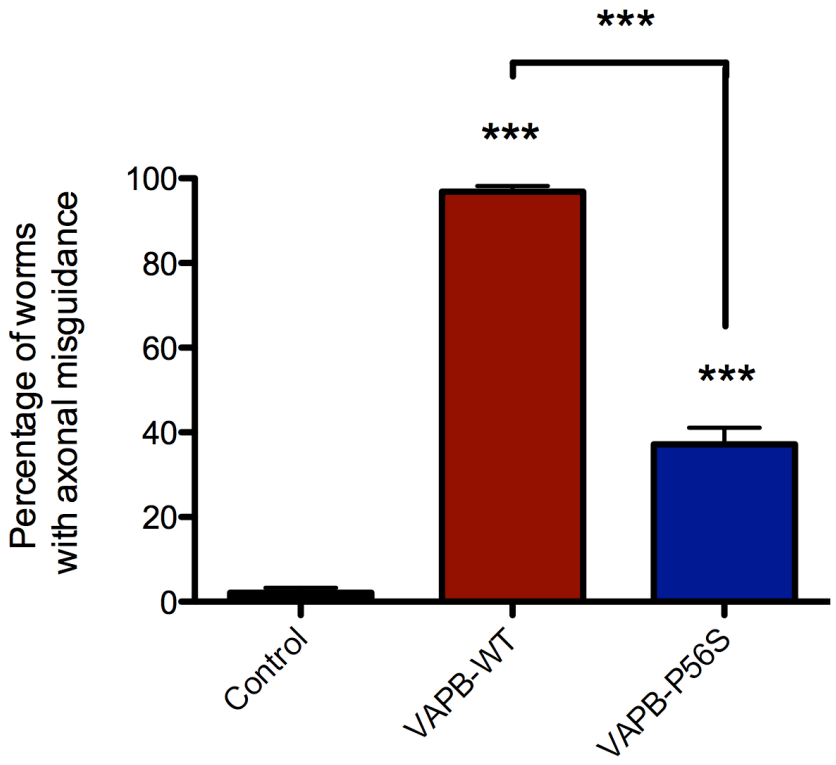

Figure 13. VAPB-WT and VAPB-P56S worms have a high frequency of one or more misguided DA and DB motor neurons.

Misguided axons from the DA and DB neurons can be visualized (Day 3). For each VAPB transgenic strain, an average of 150 worms were quantified. The frequency of worms with one or more misguided axons is given as a percentage ± S.E. Compared to control (2.1% ± 1.2), VAPB-WT and VAPB-P56S have significantly higher incidences of misguidance at 96.9% ± 1.4% S.E. (***, $p<0.001$) and 37.2% ± 4.0% S.E. ($p<0.001$) respectively. Also, VAPB-WT has a higher frequency of misguidance than VAPB-P56S ($p<0.001$). Statistical analyses using a One-way ANOVA followed by a post-hoc Bonferroni test were performed.

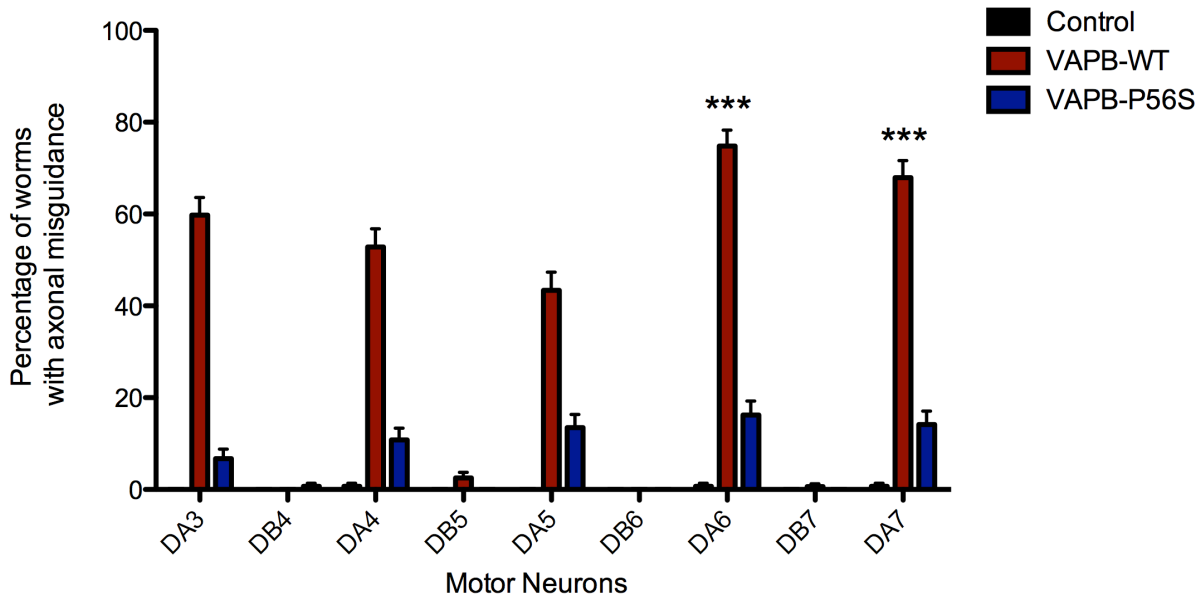

Figure 14. DA6 and DA7 motor neurons are most susceptible to axonal misguidance in VAPB-WT worms.

Misguided axons from the DA and DB neurons can be visualized (Day 3). For each VAPB transgenic strain, an average of 150 worms were quantified. The specificity of axonal misguidance in DA and DB motor neurons of VAPB transgenic *C. elegans* strains was quantified, and the frequency of misguidance is given as a percentage ± S.E. Compared to other DA and DB neurons, DA6 and DA7 were the most susceptible in VAPB-WT worms (***, $p<0.001$). 74.8% ± 3.4% S.E. of VAPB-WT worms had misguided DA6 neurons, and 67.9% ± 3.7% S.E. of VAPB-WT worms had misguided DA7 neurons. There was little to no misguidance seen in the DB motor neurons or control. Statistical analyses using a Two-way ANOVA followed by a post-hoc Bonferroni test were performed.

VAPB-WT and VAPB-P56S expression induce age-dependent neuronal loss

Premature neuronal death and the progressive loss of upper and lower motor neurons in the cortex, brain stem and spinal cord are characteristic of ALS. However, with the exception of a recent overexpression mouse model developed by Aliaga and colleagues, which was the first to show any motor neuron death with evidence of progressive loss of corticospinal motor neurons mainly in the motor cortex (Aliaga et al., 2013), previous animal models fail to display evidence of motor neuronal death. As with many neurodegenerative diseases, symptoms appear later despite the fact that the inherited mutation exists throughout life. This gives rise to the notion of an increased vulnerability with age or a trigger due to an accumulation of other factors. To explore whether there is age-dependent loss, neuronal loss was quantified at various stages of the worm's adult life.

Since DA neurons can be visualized using the DA and DB specific *unc-129p::GFP* reporter (Colavita et al., 1998), this allowed the assessment of motor neuronal death of these specific neurons. The DA and DB motor neurons in each transgenic *C. elegans* strain were assessed for age dependent neuronal loss at Day 3, 7, 11 of adulthood. Whenever the cell body and commissures of a DA or DB motor neuron were not visible, the lack of GFP was scored as neuronal loss (or a non-visible neuron).

On Day 3 of adulthood, the frequency of worms with one or more non-visible neurons (scored as motor neuronal loss) was higher in VAPB-WT (32.1% ± 3.7%) than control (4.2% ± 1.7%) or VAPB-P56S (16.2% ± 3.0%); and the VAPB-P56S worms exhibited a higher incidence of neuronal loss compared to control. By Day 11, VAPB-WT (64.3% ± 4.8%) was still the strain with the highest percentage of worms exhibiting

evidence of neuronal loss compared to the control (12.1% ± 3.6%) and VAPB-P56S worms (43.8% ± 4.5%).

There was little loss observed in control strains and no statistically significant increase from Day 3 to 11 (4.2% ± 1.7% to 12.1% ± 3.6% respectively, $p>0.05$). However, there were significant increases in the overall frequency of neuronal loss in the VAPB-P56S strain from Day 3 to 7 (from 16.2% ± 3.0% to 30.3% ± 4.2%, $p<0.01$) and Day 7 to 11 (30.3% ± 4.2% to 43.8% ± 4.5%, $p<0.01$). In the VAPB-WT worms, there was no significant increase in neuronal loss from Day 3 to Day 7. However, there was significant loss of DA neurons from Day 7 to 11 (40.8% ± 4.3% to 64.3% ± 4.8%, $p<0.001$) (Figure 15). The increases in the loss of DA neurons of VAPB-WT and VAPB-P56S strains from Day 3 to 11 suggest that expressing the human VAPB genes in the DA neurons leads to age-dependent neuronal loss. This loss was restricted to DA neurons as DB neurons were largely unaffected. Of the DA neurons, DA6 and DA7 appeared to be the most susceptible to age-dependent loss, with an increase seen from Day 3 to 11 in both VAPB-WT and VAPB-P56S strains (Figure 16).

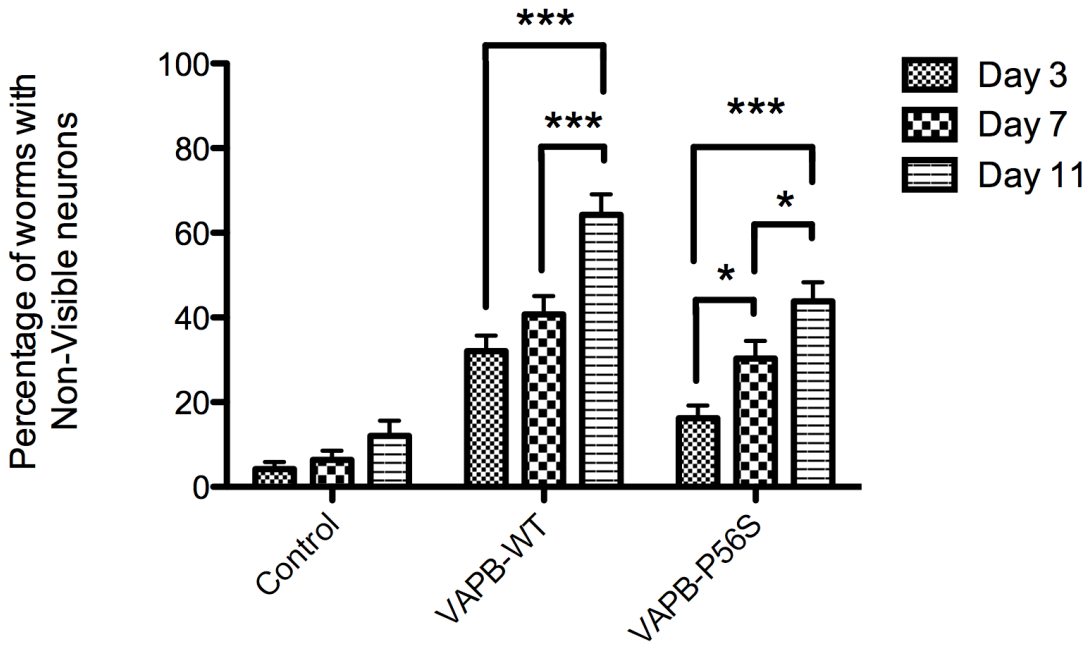

Figure 15. VAPB-WT and VAPB-P56S worms exhibit age-dependent motor neuronal loss from Day 3 to Day 11 of adulthood.

The axons and cell bodies of DA and DB neurons can be visualized (Day 3, 7, 11). For each VAPB transgenic strain, an average of 125 worms was quantified. The frequency of worms with one or more non-visible DA or DB motor neuron at Day 3, 7, 11 of adulthood is given as a percentage ± S.E. A significant increase in worms with one or more non-visible DA or DB neurons was seen in VAPB-WT worms from Day 7 to 11 (40.8% ± 4.3% S.E. to 64.3% ± 4.8% S.E., [***, $p<0.001$]) and from Day 3 to 7 (*, $p<0.05$) as well as Day 7 to 11 (30.3% ± 4.2% S.E. to 43.8% ± 4.5% S.E., [*, $p<0.05$]) in VAPB-P56S worms. Very little loss was observed in control strain. Statistical analyses using a Two-way ANOVA followed by a post-hoc Bonferroni test were performed.

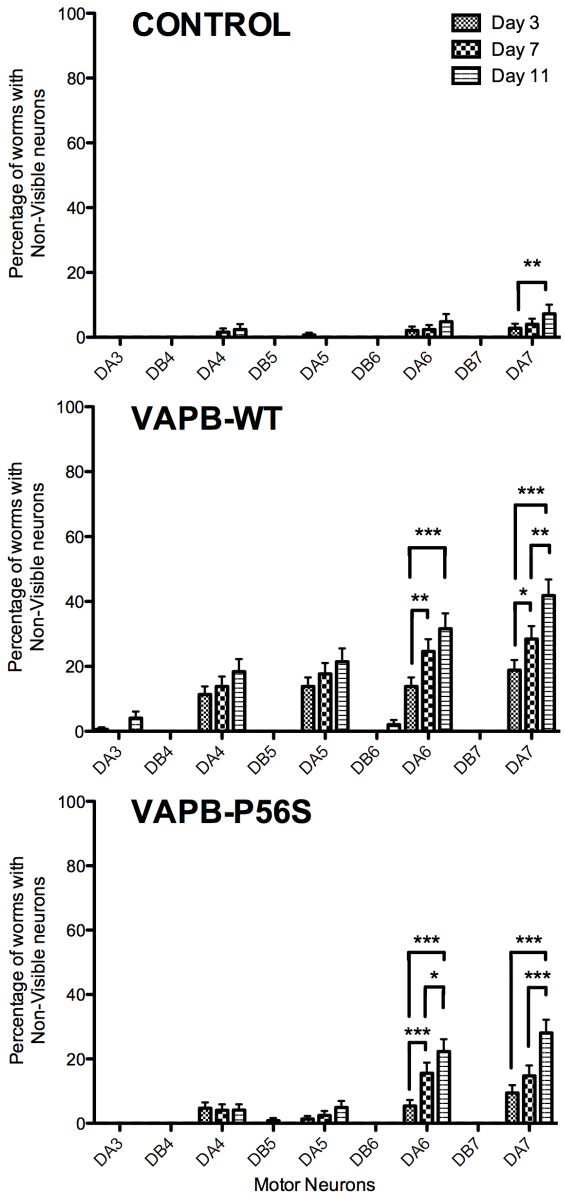

Figure 16. DA6 and DA7 motor neurons are most susceptible to age-dependent neuronal loss from Day 3 to Day 11 of adulthood.

The axons and cell bodies can be visualized (Day 3, 7, 11). For each VAPB transgenic strain, an average of 125 worms was quantified. The specificity of non-visible DA and DB motor neurons of VAPB transgenic *C. elegans* strains was quantified, and the frequency of non-visible neurons is given as a percentage ± S.E. DA6 and DA7 were the most susceptible to age-dependent loss in VAPB-WT worms and VAPB-P56S worms (***, $p<0.001$; **, $p<0.01$; *, $p<0.05$). There was little to no loss seen in DB motor neurons or control. Statistical analyses using a Two-way ANOVA followed by a post-hoc Bonferroni test were performed.

VAPB-WT expression leads to a reduced lifespan relative to control and VAPB-P56S

Generally, ALS patients are diagnosed in the 40^{th} to 60^{th} decades of their lives and they succumb to respiratory failure within two to five years of symptom-onset (Boillee et al., 2006). For ALS8 patients in particular, some may face a rapid and severe progression whereas others experience a slow progression that takes decades (Mitne-Neto et al., 2011) after the initial onset of disease between 25-55 years of age.

Since expressing human VAPB-P56S and VAPB-WT in the DA neurons caused locomotor defects, axonal misguidance and age-dependent neuronal loss, the lifespans of these transgenic strains were also assessed. For the lifespan assay, adult transgenic worms were maintained on 120 μM FUDR agar plates for 5 days before transferring them back to regular NGM agar plates until the end of their lifespan. Because FUDR is an antimetabolite that inhibits DNA synthesis, the embryos laid by the adult worms did not hatch, which allowed for examination of the original adult transgenic worms throughout their lifespan. Survival curves were produced and compared using the Log-rank (Mantel-Cox) test (Figure 17).

While the average longest living control was 31 days and 32 days for VAPB-P56S worms, the maximum lifespan for VAPB-WT worms was 23 days. This indicates that VAPB-WT expression leads to a reduced lifespan relative to control and VAPB-P56S strains ($p<0.001$).

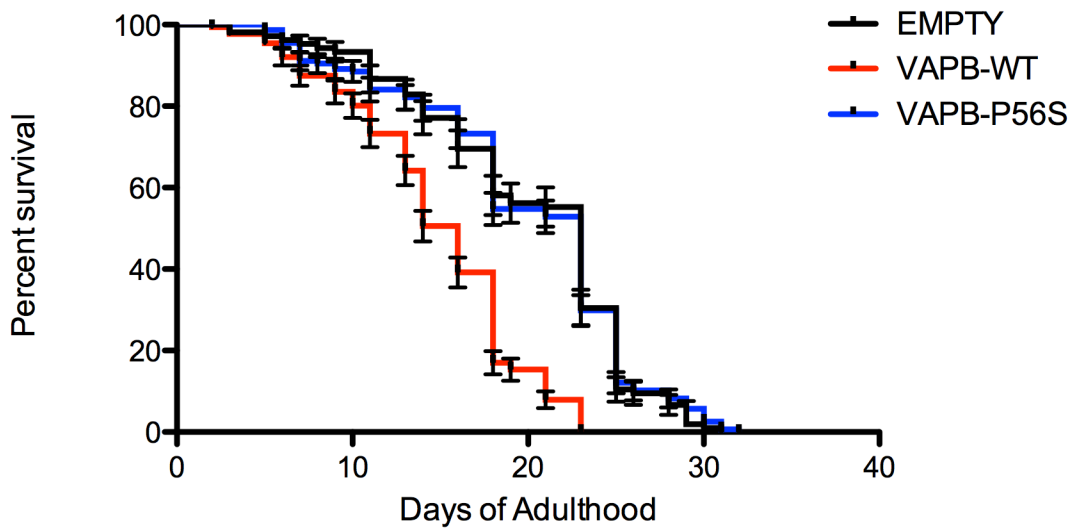

Figure 17. VAPB-WT expression in DA neurons reduces adult lifespan in *C. elegans.*

DA neurons express FLAG-tagged human VAPB-WT and FLAG-tagged human VAPB-P56S. The VAPB-WT strain has a reduced lifespan relative to the control and VAPB-P56S worms, assayed at 22 °C. Lifespan curves are based on an average of 145 worms per strain. Survival curves were produced and compared using the Log-rank (Mantel-Cox) test ($p<0.001$).

Increased frequency of neuronal loss following Paraquat treatment by Day 7 and Day 11

In cellular studies, the expression of VAPB-P56S leads to two main changes in the cell. Not only does expressing the mutant VAPB result in a loss of the characteristic reticular structure of the ER (Kanekura et al., 2006), it also leads to a loss of the integrity of the nuclear envelope (Tran et al., 2012). Since VAPB-P56S is implicated in ER stress and the deterioration of the nuclear envelope, it is possible that an additional stress is required to trigger neuronal death. Thus, the potential enhanced vulnerability of neurons to oxidative stress was tested.

Paraquat is a non-selective, widely used bipyridyl herbicide that is a prototypical agent for experimental generation of reactive oxygen species (ROS) (Drechsel and Patel, 2009). The VAPB transgenic worms were treated with 7.5 mM Paraquat for 17-hours at Day 1 of adulthood and transferred to regular NGM agar plates the subsequent day. The worms were then scored for neuronal loss at Day 3, 7 or 11 of adulthood.

Following Paraquat treatment, there was an overall increase in the percentage of worms with one or more non-visible neurons by Day 3 of adulthood in the VAPB-WT and VAPB-P56S worms (Figure 18). Treating the worms with Paraquat increased the incidence of worms exhibiting neuronal loss by at least 10% in Day 3 VAPB-WT ($p<0.001$) and VAPB-P56S worms ($p<0.001$). However, in the VAPB-P56S strain, although the increase in the percentage of worms with neuronal loss following treatment was significant in Day 7 worms ($p<0.01$), it was not significant for Day 11 adults ($p>0.05$). Further, there were no considerable increases in the percentage of control worms with neuronal loss following treatment by Day 3 or 11, with the exception of a

slight but significant increase at Day 7 ($p<0.05$).

In terms of specificity, DA6 and DA7 appeared to be the most susceptible to age-dependent neuronal loss following Paraquat treatment in VAPB-WT and VAPB-P56S strains (Figure 19). There was a considerable increase in incidences of VAPB-WT worms losing DA7 neurons by Day 7 ($p<0.001$) and Day 11 ($p<0.01$) following treatment compared to the untreated control. This was also observed between treated and untreated VAPB-P56S worms at Day 7 ($p<0.01$) and Day 11 ($p<0.001$). DA6 neurons in the VAPB-P56S strain also exhibited a significant loss ($p<0.05$) between untreated and treated conditions by Day 7 of adulthood. Regardless of the treatment condition, DB neurons were largely unaffected across all strains at each measured stage. Together, this suggests that the expression of VAPB-WT and VAPB-P56S enhances the vulnerability of DA neurons to oxidative stress, and DA6 and DA7 are the most vulnerable of the DA neurons.

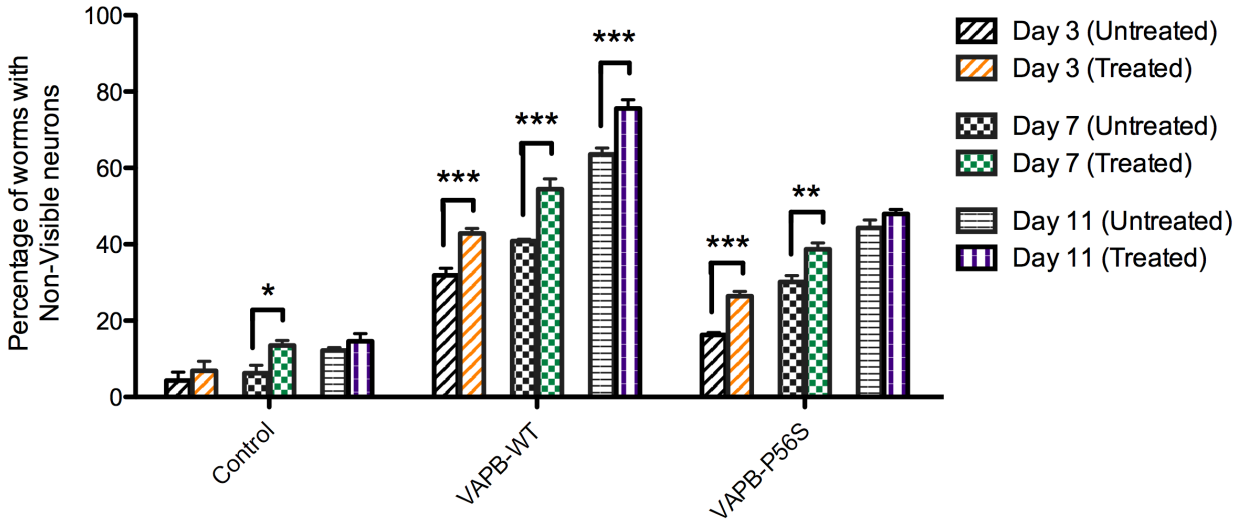

Figure 18. Frequency of transgenic VAPB strains with one or more non-visible DA or DB motor neurons at Day 3, 7, 11 of adulthood following Paraquat treatment.

Worms were treated acutely with Paraquat at Day 1 and assessed at Day 3, 7, 11. For each VAPB transgenic strain, an average of 125 untreated transgenic worms and 86 treated transgenic worms were quantified. The frequency of worms with non-visible neurons is given as a percentage ± S.E. There were significant increases in the frequency of VAPB-WT worms with one or more non-visible DA and DB neurons following Paraquat treatment by Day 3, 7, 11 of adulthood (***, $p<0.001$). Day 7 and 11 VAPB-P56S worms also exhibited significant increases following treatment (**, $p<0.01$). However, other than a slight increase by Day 7 (*, $p<0.05$), there were insignificant increases in the frequency of control worms with neuronal loss, regardless of treatment. Statistical analyses using a Two-way ANOVA followed by a post-hoc Bonferroni test were performed.

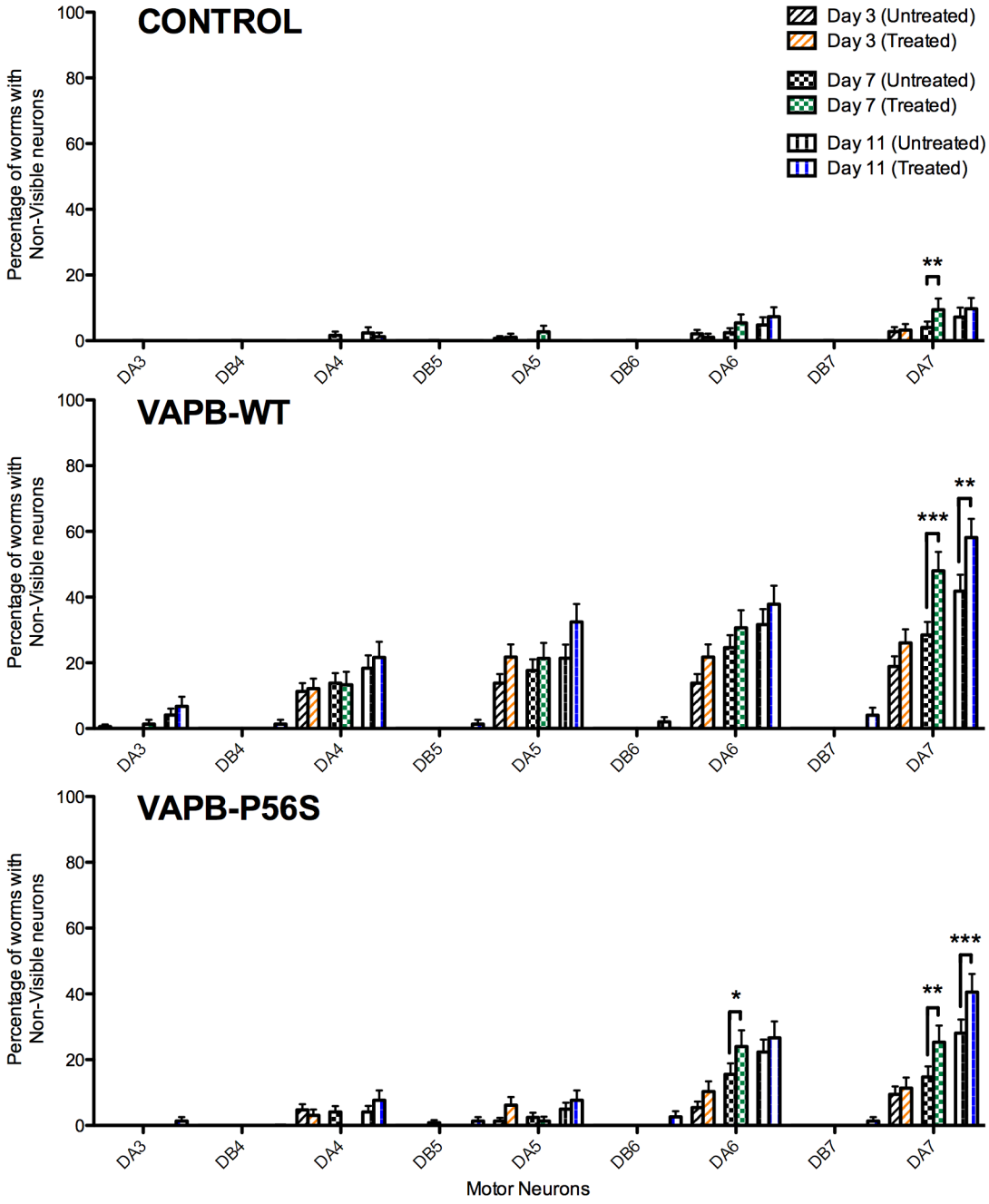

Figure 19. DA6 and DA7 motor neurons are most susceptible to age-dependent neuronal loss following Paraquat treatment by Day 7 and 11 of adulthood.

Worms were treated acutely with Paraquat at Day 1 and assessed at Day 3, 7, 11. For each VAPB transgenic strain, an average of 125 untreated transgenic worms and 86 treated transgenic worms were quantified. The specificity of non-visible DA and DB motor neurons of VAPB transgenic *C. elegans* strains was quantified, and the frequency

of non-visible neurons is given as a percentage ± S.E. Compared to other DA and DB neurons, DA6 and DA7 of VAPB-P56S worms were the most susceptible to loss following treatment by Day 7 and Day 11 (***, $p<0.001$; **, $p<0.01$; *, $p<0.05$). DA7 of VAPB-WT was the most vulnerable following treatment by Day 7 and 11. There was little to no loss seen in DB motor neurons or control strain. Statistical analyses using a Two-way ANOVA followed by a post-hoc Bonferroni test were performed.

vpr-1(RNAi) Knockdown Transgenic Strain

vpr-1 knockdown in DA neurons results in a slower rate and increased uncoordination in backward locomotion by Day 6

Previous studies have shown decreased levels of VAPB in spinal cords of ALS patients (Anagnostou et al., 2010) as well as in motor neurons derived from iPSCs of ALS8 patients (Mitne-Neto et al., 2011). Further, the current view of autosomal dominant ALS8-linked VAPB-P56S is that it is aggregate prone (Suzuki et al., 2009) and acts in a dominant negative fashion by dimerizing with endogenous VAPB-WT (Teuling et al., 2007). Together, this indicates that VAPB-P56S is a loss of function mutation. To recapitulate this pathogenic mechanism, a second *C. elegans* model was generated by knocking down *vpr-1,* the *C. elegans* ortholog of VAP. Because knocking out *vpr-1* is embryonic lethal and the neurons of *C. elegans* are resistant to RNAi knockdown via feeding (Asikainen et al., 2005), a transgenic worm was created by microinjection. RDE-1, an Argonaute protein essential for RNAi, activity was reconstituted in the DA neurons of an *rde-1* null mutant worm by placing it under the control of an *unc-4* promoter. As described in the Materials and Methods, a plasmid with *hsp-16p* driving *vpr-1 sense* and *anti-sense* was used to induce *vpr-1* knockdown specifically in the DA neurons upon heat shock, as all other cells lack RDE-1 expression. The control worms did not have RDE-1 reconstituted in the DA neurons and thus, *vpr-1* was not knocked down even with heat shock. The worms were assessed for motor deficits, such as a locomotor defect, through a reversal behavior assay. *C. elegans* either reverse randomly or immediately upon stimulus. Therefore, a fine platinum wire was used to induce an immediate reversal in *C. elegans* locomotion and subsequent backward locomotion was analyzed.

During early adulthood (Day 3), the rates of backward locomotion of both the control (0.77 ± 0.04 turns/second) and *vpr-1(RNAi)* (0.75 ± 0.04 turns/second) were very similar. Heat shocking the control strain had no effect on the rate of backward locomotion of the Day 3 control worms (0.77 ± 0.04 turns/second) as they moved backwards at an identical rate to the non-heat shocked Day 3 worms. Following heat shock induced knockdown of *vpr-1,* there was no significant change in the rate of backward locomotion of Day 3 *vpr-1(RNAi)* worms (0.77 ± 0.05 turns/second). Regardless of either heat shock inducing *vpr-1* knockdown in DA neurons or not, the rate of backward locomotion remained unchanged at Day 3 of adulthood (Figure 20).

In all cases, as the worms age, their backward locomotion rates slowed considerably as shown by the rates of the control and *vpr-1(RNAi)* at Day 6 (0.48 ± 0.02 turns/second and 0.40 ± 0.02 turns/second, respectively) compared to Day 3 of adulthood (Figure 20). Focusing on the slower Day 6 adults, there is a significant difference between the *vpr-1(RNAi)* worms that underwent heat shock induced *vpr-1* knockdown compared to non-heat shocked worms. Following the knockdown of *vpr-1,* the rate of backward locomotion of Day 6 *vpr-1(RNAi)* worms was over four times slower than Day 6 *vpr-1(RNAi)* worms without heat shock-induced *vpr-1* knockdown (0.09 ± 0.01 turns/second compared to 0.40 ± 0.02 turns/second, respectively, $p<0.001$). On the other hand, control at Day 6 of adulthood moved backwards at a similar rate regardless of whether the strain was heat shocked or not (0.48 ± 0.03 turns/second and 0.48 ± 0.02 turns/second, $p>0.05$). Day 6 *vpr-1(RNAi)* without the induction of *vpr-1* knockdown was not significantly different from these rates (0.40 ± 0.02 turns/second, $p>0.05$).

In addition to the slowed rate of backward locomotion following heat shock induced *vpr-1* knockdown in DA neurons, an abnormal locomotion phenotype was also observed during the reversal behavior assays when the worms were prodded to move backwards. Upon prodding, *C. elegans* typically move in an undulating, sinusoidal fashion backwards away from the stimulus (Gray and Lissmann, 1964). However, some worms exhibited characteristic uncoordinated phenotypes, such as coiling or partial body movements.

When the strains were younger, during Day 3 adulthood, the frequency of worms with uncoordinated backward locomotion was low. In control worms, little to no incidences of uncoordination was observed with only 3.9% ± 3.8% of non-heat shocked and heat shocked worms exhibiting this abnormal behavior. Heat shock-induced knockdown of *vpr-1* did not increase the frequency of uncoordination during early adulthood (Day 3). However, by Day 6, 59.8% ± 5.4% of heat shocked *vpr-1(RNAi)* worms showed uncoordinated phenotypes of coiling or partial body movements (Figure 21). This is significantly higher than Day 6 non-heat shocked *vpr-1(RNAi)* worms (15.9% ± 4.0%, $p<0.001$) and both non-heat shocked and heat shocked control strains (6.3% ± 2.7% and 13.6% ± 3.8%, respectively). There was no significant difference between heat shocked and non-heat shocked control. The uncoordinated phenotype was highest in Day 6 worms when *vpr-1* was knocked down ($p<0.001$) (Figure 22).

This data indicates that the locomotor defects, uncoordination and slowed rate of backward locomotion, are not only age-dependent but also dependent on the knockdown of *vpr-1*.

(Refer to Appendix A for video of the backward locomotion.)

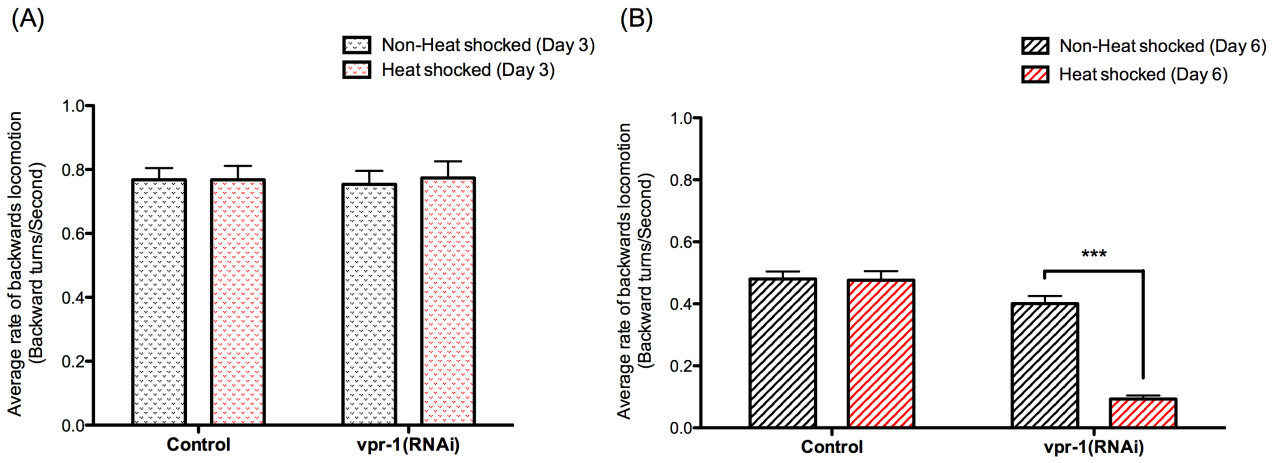

Figure 20. *vpr-1* knockdown in DA neurons results in a slowed rate of backward locomotion by Day 6 (B).

The average rate of backward locomotion of Day 3 (A) and Day 6 (B) *vpr-1(RNAi)* knockdown strain following stimulus is shown. The behavioural assay was conducted by a harsh-touch method to the head of each adult *C. elegans* (Day 3 and 6 adults) directly behind the pharynx, and its initial backward movement before returning to its forward motion was recorded. Since *C. elegans* move in a distinct sinusoidal motion, one full "body turn" was defined as half a wavelength of a sine wave (π). For each knockdown strain, an average of 81 Day 6 worms was quantified. The rate of backward locomotion is given as the mean rate ± S.E.M. As each strain ages (from Day 3 to Day 6), their backward locomotion slows. Compared to the control and the non-heat shocked *vpr-1(RNAi)*, heat shock *vpr-1* knockdown of Day 6 *vpr-1(RNAi)* exhibited slower rates of 0.09 backward turns/second ± 0.01 S.E.M. (***, $p<0.001$). Statistical analyses using a Two-way ANOVA followed by a post-hoc Bonferroni test were performed.

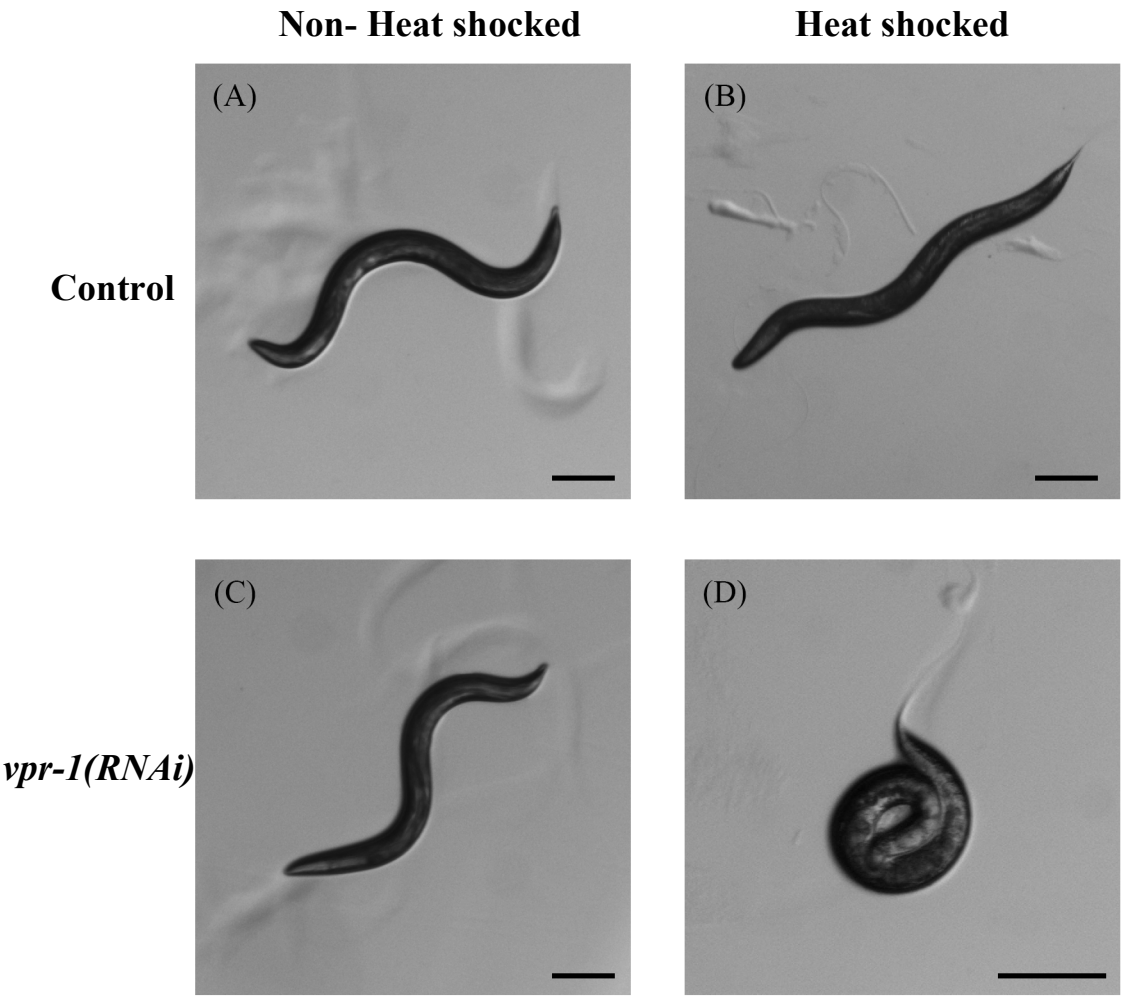

Figure 21. *vpr-1* knockdown in DA neurons leads to increased uncoordinated backward locomotion by Day 6 of adulthood.

A reversal behavior assay was conducted by a harsh-touch method to the head of each adult *C. elegans* directly behind the pharynx, and its initial backward movement before returning to the forward direction was observed for uncoordinated movement. Coiling up or only partial body movement was defined as 'uncoordination'. Day 6 *vpr-1(RNAi)* worms with heat shock induced *vpr-1* knock down exhibited the most frequent uncoordination (D), whereas non-heat shocked *vpr-1(RNAi)* along with non-heat shocked and heat shocked control reversed in a sinusoidal motion (A-C). Scale bar = 100 μm.

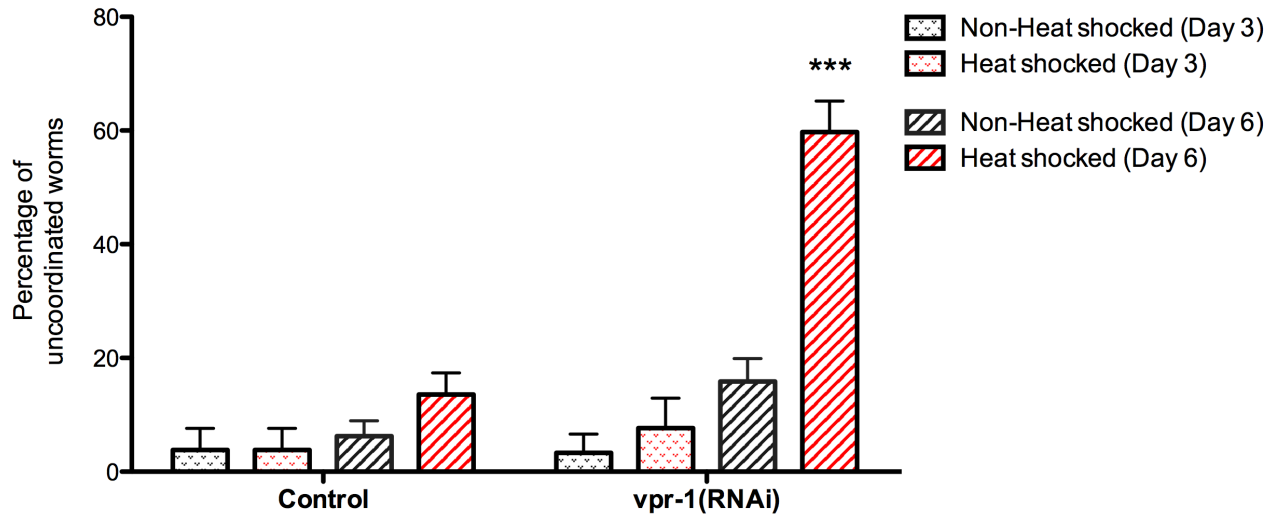

Figure 22. *vpr-1* knockdown in DA neurons leads to increased uncoordinated backward locomotion by Day 6 of adulthood.

The percentage of worms exhibiting uncoordinated backward locomotion at Day 3 and Day 6 of adulthood following stimulus is shown. A reversal behaviour assay was conducted by a harsh-touch method to the head of each adult *C. elegans* directly behind the pharynx, and its initial backward movement before returning to the forward direction was observed for uncoordinated movement. Coiling up or only partial body movement was defined as 'uncoordination'. For each knockdown strain, an average of 81 Day 6 worms was quantified. The frequency of uncoordinated worms is given as a percentage ± S.E. Although few incidences of uncoordination was observed in Day 3 adult worms regardless of heat shock, heat shock *vpr-1* knockdown of Day 6 *vpr-1(RNAi)* lead to 59.8% ± 5.4% S.E. of worms exhibiting uncoordinated backward locomotion (***, $p<0.001$). Statistical analyses using a Two-way ANOVA followed by a post-hoc Bonferroni test were performed.

vpr-1 knockdown in DA neurons induces age-dependent neuronal loss

Since the general consensus is that the pathogenic mechanism for ALS8 is a loss of function mutation, age-dependent neuronal loss was assessed following *vpr-1* knockdown in the *vpr-1(RNAi)* strain during its short, approximate 14 day life cycle.

Since the *vpr-1(RNAi)* strains were crossed with *unc-129p::GFP*, which expresses GFP in the DA and DB motor neurons (Colavita et al., 1998), the DA neurons could be readily visualized (Figure 23A), which allowed for the assessment of motor neuronal death of these specific neurons at various stages of the worm's adult life. Whenever the cell body and commissures of a DA or DB motor neuron were not visible, the lack of GFP was scored as neuronal loss (or a non-visible neuron). Figure 23B shows a Day 6 heat shocked control worm with DA and DB neurons shown and Figure 23C shows a Day 6 heat shock induced *vpr-1* knockdown worm (*vpr-1(RNAi))* missing DA6 and DA7, as shown by the arrowheads.

By Day 3 of adulthood, irrespective of heat shock, neither control nor *vpr-1(RNAi)* strains showed significant differences in the incidence of DA neuronal loss observed in the worms. Knocking down *vpr-1* by heat shock in *vpr-1(RNAi)* did not increase the percentage of worms with one or more DA neurons lost (Figure 24). However, by Day 6 of its adult life, the frequency of worms with one or more non-visible DA neurons (scored as motor neuronal loss) was significantly higher in *vpr-1(RNAi)* worms following the induction of *vpr-1* knockdown (30.9% ± 4.2%) compared to the same strain without the heat shock induction of *vpr-1* knockdown (5.3% ± 1.8%, $p<0.001$). Additionally, control worms exhibited only low frequencies of DA neuronal loss at Day 6 with or without heat shock-induced vpr-1 knockdown (2.2% ± 1.2% and

1.4% ± 1.0%, respectively) (Figure 24). This suggests that the loss of DA neurons is not only dependent on the knockdown of *vpr-1* but is also age-dependent.

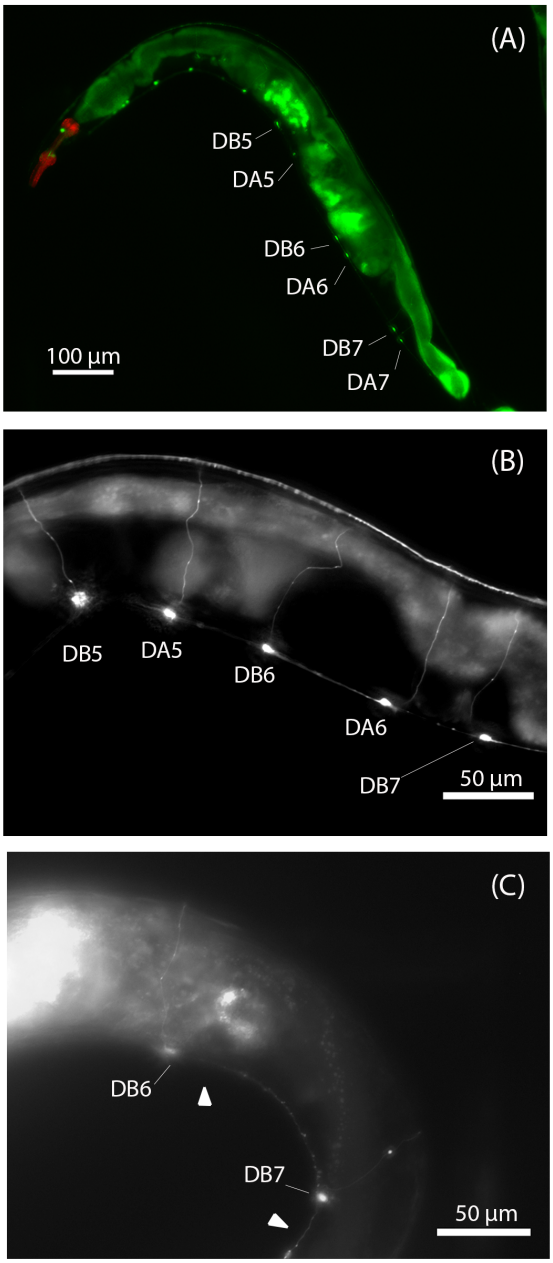

Figure 23. DA and DB neurons in *vpr-1(RNAi)* knockdown *C. elegans* at Day 6 of adulthood.

The ventral cord DA and DB neurons innervate dorsal muscles. The axons and cell bodies of DA and DB neurons of the heat shocked control (A-B) and heat shocked *vpr-1(RNAi)* (C) are shown. The transgenic knockdown worms were crossed with *unc-129p::GFP* for visualization of the axons and cell bodies. Arrowheads represent missing DA neurons.

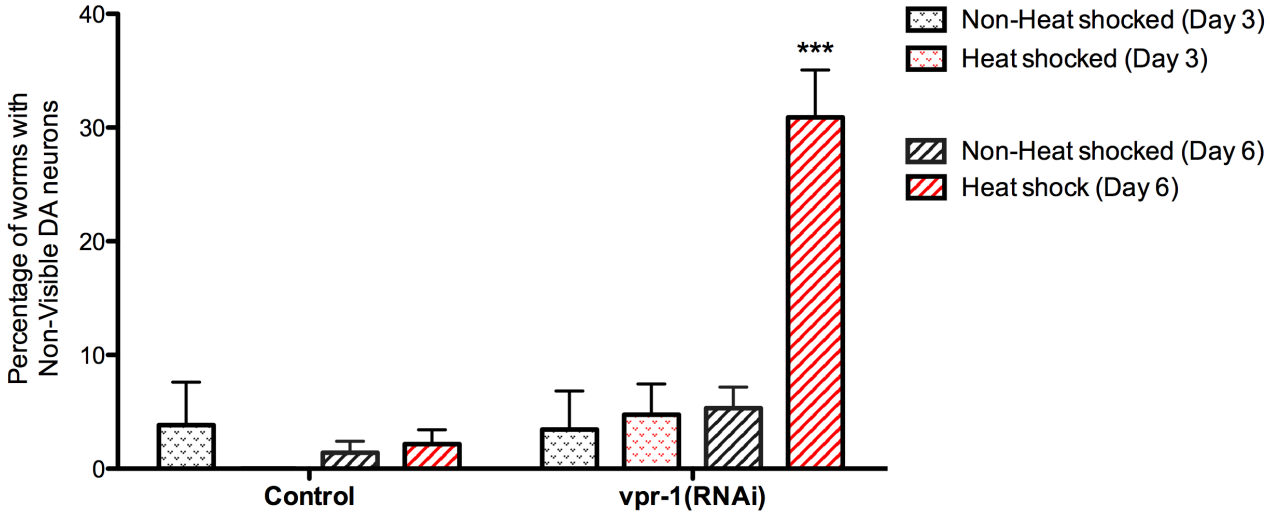

Figure 24. *vpr-1* knockdown in DA neurons induces age-dependent neuronal loss by Day 6 of adulthood.

The axons and cell bodies of DA and DB neurons can be visualized (Day 3, 6). For each *vpr-1* knockdown strain, an average of 87 worms was quantified. The frequency of worms with one or more non-visible DA motor neurons at Day 3 or 6 of adulthood is given as a percentage ± S.E. A significant increase in the number of worms with one or more non-visible DA neurons was seen in heat shocked *vpr-1* knocked down *vpr-1(RNAi)* worms by Day 6 (30.89% ± 4.17% S.E. [***, $p<0.001$]). Very little loss was observed at Day 3 or in the Day 6 control and non-heat shocked *vpr-1(RNAi)*. Statistical analyses using a Two-way ANOVA followed by a post-hoc Bonferroni test were performed

DA6 and DA7 neurons are most susceptible to neuronal loss following vpr-1 knockdown in DA neurons by Day 6

The posterior DA neurons, DA6 and DA7 appear to be the most susceptible to age-dependent neuronal loss following the heat shock induction of *vpr-1* knockdown in *vpr-1(RNAi*) strains by Day 6 of adulthood (16.26% ± 3.32% and 17.89% ± 3.46%, respectively). The frequency of worms exhibiting DA6 or DA7 loss was significantly higher than any percentage observed in other DA or DB neurons in the control or *vpr-1(RNAi*) worms with or without the heat shock induction of *vpr-1* knockdown (Figure 25). The enhanced susceptibility of the posterior DA neurons, DA6 and DA7, is also consistent with the VAPB transgenic worms.

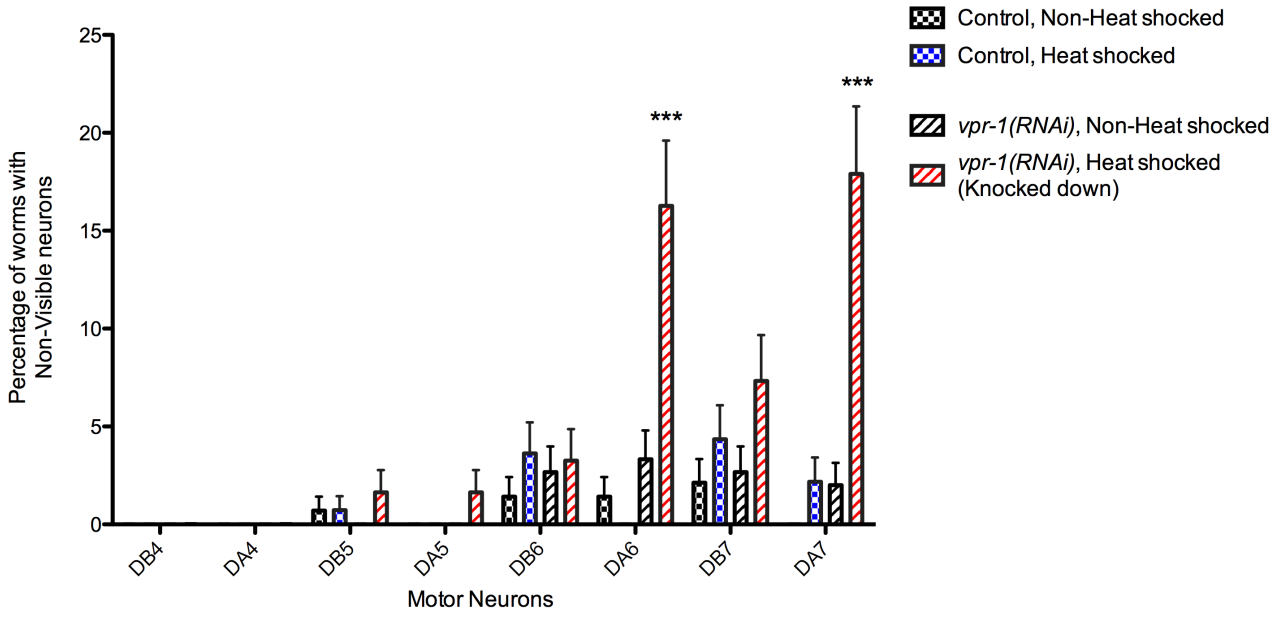

Figure 25. DA6 and DA7 motor neurons are most susceptible to neuronal loss following *vpr-1* knockdown in DA neurons by Day 6 of adulthood.

For each condition and strain, an average of 138 worms (Day 6) was quantified. The specificity of non-visible DA and DB motor neurons of *vpr-1* knockdown *C. elegans* strains was quantified, and the frequency of non-visible neurons is given as a percentage ± S.E. Compared to other DA and DB neurons, DA6 and DA7 were the most susceptible to loss in *vpr-1(RNAi)* worms following heat shock induced *vpr-1* knockdown (***, $p<0.001$). There was little to no loss seen in DB motor neurons, control, or non-heat shocked *vpr-1(RNAi)*. Statistical analyses using a Two-way ANOVA followed by a post-hoc Bonferroni test were performed.

DISCUSSION

First described in 2004 and initially mapped in a Brazilian family, ALS8 is a late-onset, autosomal dominant form of familial ALS that is characterized by a VAPB-P56S mutation. Although studies reveal the ubiquitously expressed, aggregate-prone, dominant negative VAPB-P56S causes two main structural changes in the ER and nuclear envelope, the underlying mechanism contributing to neuronal death and the selective vulnerability of the motor neurons is unknown. However, due to investigations of spinal cord samples of ALS patients (Anagnostou et al., 2010) and motor neurons derived from iPSCs of ALS8 patients (Mitne-Neto et al., 2011), the general consensus is that ALS8-linked VAPB-P56S pathogenesis is a loss of function mutation.

Multiple animal models of ALS8, from *Drosophila* to zebrafish to mice, have been created to either overexpress human VAPB-P56S or ablate the VAP ortholog. Unfortunately, with the exception of an overexpression mouse model showing evidence of progressive loss of corticospinal motor neurons in the motor cortex (Aliaga et al., 2013), previous animals do not exhibit age-dependent neuronal loss. Thus, the primary goal of this study was to generate a *C. elegans* model for mutant VAPB-P56S, characterizing the role of VAPB in motor neurons, and to show evidence of motor neuron death. Two different *C. elegans* models, an overexpression of human VAPB-P56S and knockdown of the VAP ortholog, were created and analyzed for motor deficits, age dependent neuronal loss and the selective vulnerability of specific neurons.

Human VAPB Transgenic *C. elegans* Model

Human VAPB transgenic C. elegans exhibit a slowed rate of backward locomotion, axonal misguidance, vulnerability to oxidative stress, and age-dependent neuronal loss

Clinically heterogeneous, ALS is characterized by the progressive degeneration of motor neurons that innervate voluntary muscle, including upper motor neurons in the cerebral cortex and lower motor neurons in the medulla and anterior horn of the spinal cord. The loss of lower motor neurons leads to common clinical features such as fasciculation, cramps, weakness in the limbs and muscle atrophy. In about two-thirds to three quarters of patients, ALS begins in the limbs, spinal-onset, while the rest of ALS cases are bulbar-onset (Gordon, 2013; Turner et al., 2010). The initial symptoms of limb-onset include limb function deterioration such as foot drop, difficulty walking and the loss of dexterity or weakness in lifting the arms (Chio et al., 2009). ALS8 patients generally experience limb and trunk weakness with decreased or absent deep-tendon reflexes along with muscular cramps and fasciculation (Nishimura et al., 2004b).

Although the first mouse model for ALS8 in 2010 overexpressing VAPB-P56S in the nervous system did not show an overt motor phenotype (Tudor et al., 2010b), a transgenic mouse model created in 2013 overexpressing human VAPB-P56S heterologously under a stronger *Thy1.2* pan-neuronal promoter exhibited motor abnormalities similar to human cases of ALS. At 2 months of age, the VAPB-P56S mice exhibited a gait abnormality, depicted by a shortened stride length and time that, however, did not worsen with age. Although there was no difference observed through grip tests, rotarod tests showed deficits in motor coordination and balance by 12 months

(Aliaga et al., 2013). Likewise, the locomotion of the transgenic *C. elegans* model overexpressing human VAPB-P56S was analyzed.

C. elegans are nematodes that normally move in an undulating, sinusoidal motion (Gray and Lissmann, 1964) and reverse randomly or immediately upon stimulus to a backward-directed locomotion, which consists of the propagation of dorsoventral body bends from the posterior to the anterior (Gray et al., 2005). To determine if human VAPB-P56S expression leads to motor abnormalities observed in previous animal models and human ALS cases, the gene was expressed in DA neurons, which control backward locomotion. Backward-directed locomotion was chosen because forward-directed locomotion is essential to survival and any possible locomotor defects could affect the worm's ability to feed (Avery & You, 2012). Reversal behavior assays revealed that both VAPB-WT worms and VAPB-P56S worms exhibited significantly slower rates of backward locomotion than the control (Figure 11). However, the decreased rate of backward-directed locomotion between VAPB-WT and VAPB-P56S worms was not significantly different. The exact mechanism causing this change in locomotion is uncertain, but a loss of the DA motor neurons controlling backward locomotion is a likely possibility. Thus, this was further analyzed at the cellular level.

C. elegans remain transparent throughout their lifecycle and by crossing VAPB transgenic worms with an *unc-129p::GFP* reporter strain, which expresses GFP in DA and DB motor neurons (Colavita et al., 1998), the axons and cell bodies of the DA and DB motor neurons were visualized easily under a fluorescence microscope for axonal misguidance. A lack of commissures and cell body was scored as neuronal loss. Although control worms exhibited the distinctive parallel axons of DA and DB motor neurons

(Figure 12A), both VAPB-WT and VAPB-P56S worms often displayed axons that did not appear to innervate the dorsal side as the commissures were mistargeted or misguided (Figure 12B and C). Quantification showed that, while both VAPB-WT and VAPB-P56S strains exhibited significantly higher incidences of worms with misguided axons compared to the control, VAPB-WT worms have the highest frequency of axonal misguidance (Figure 13). In addition to DA axonal misguidance, observations at the cellular level revealed increased frequency of DA neuronal loss at Day 3, 7 and 11 of adulthood in VAPB-WT and VAPB-P56S. The incidence of VAPB-P56S worms with a loss of one or more neurons increased progressively from Day 3 to 11, with the VAPB-WT expressing strain consistently exhibiting the highest frequency of worms with neuronal loss at each analyzed age (Figure 15). Furthermore, treating the transgenic worms with Paraquat-induced oxidative stress revealed that the DA neurons expressing VAPB-WT and VAPB-P56S had enhanced susceptibility to neuronal loss as the frequency of worms with neuronal loss in both strains increased significantly from Day 3 to 11 following a single Paraquat treatment at Day 1 (Figure 18).

Because locomotion reflects nervous system activity, along with neuronal function and structure, a motor defect such as a decreased rate of motion could be due to various factors such as muscles dysfunctioning; synapses misfiring or becoming less active; motor neurons denervating and dying; or other motor circuit problems. The exact mechanism causing the change in locomotion of the VAPB transgenic worms is uncertain but the axonal misguidance, enhanced susceptibility to oxidative stress and age-dependent neuronal loss of the DA motor neurons could be contributing factors.

The expression of VAPB-WT and VAPB-P56S in the DA neurons seemed to cause an impairment that led to mistargetting of the commissures. Since DA motor neurons are responsible for backward-directed locomotion, the increased axonal guidance defects observed in the DA motor neurons of VAPB-WT and VAPB-P56S strain, compared to the few observed defects in the control, suggests that the mistargetting of commissures from the ventral cord could affect the innervation of the muscles on the dorsal side and effectively, the undulating locomotor behavior of the worms.

Axonal misguidance in VAPB transgenic strains may be a developmental defect

Interestingly, there is no indication of axon guidance defects in human ALS8 cases and only minor axonal defects in outbranching and axonal length were observed in zebrafish that had Vapb knocked down (Kabashi et al., 2013). Thus, this finding was unforeseen, and it is possible that the axonal misguidance of DA neurons in the transgenic *C. elegans* may only be characteristic of nematodes. In *C. elegans*, the motor neurons are generated at either mid-embryogenesis or during the first larval stage (Sulston and Horvitz, 1977). The DA neurons are born just after the 300-minute mark of embryogenesis, they extend commissures to the dorsal cord during mid-embryogenesis, and are one of only three classes that are present at the ventral nerve cord upon hatching (Sulston et al., 1983). During nervous system development, axons are directed by extracellular guidance cues, such as UNC-6/netrin, Slt-1/slit, VAB-1/Eph Receptor (EphR), in order to migrate along specific pathways to reach and make functional connections with their targets. Previous studies have shown that VAB-1 EphR functions to prevent abnormal axon crossing at the ventral midline (Zallen et al., 1999) and mutations in EphR cause defects in cell and axon guidance during development (Klein,

2004). VAP MSP domains appear to act as secreted ligands for Eph receptors as well and the loss of VPR-1, the VAP ortholog in *C. elegans,* causes defects in distal-tip cell (DTC) migration (Tsuda et al., 2008). It is also believed that the P56S mutation in the MSP domain of VAPB prevents MSP secretion (Tsuda et al., 2008). Therefore, *unc-4p* driven overexpression of VAPB-WT and VAPB-P56S expression in the DA neurons could potentially interfere with signaling and, subsequently cause axonal mistargetting of the DA neurons during development.

Axonal misguidance and increased vulnerability to oxidative stress may contribute to DA neuronal loss in VAPB transgenic strains

There appeared to be a possible correlation between axonal misguidance and neuronal loss in the VAPB transgenic strains as the strain that displayed a higher frequency of worms with axonal misguidance also had a higher frequency of worms with DA neuronal loss. Similar frequencies were observed in VAPB-P56S worms exhibiting axonal misguidance and neuronal loss by Day 11. However, this correlation was not as prominent in VAPB-WT worms as the percentage of worms with misguided DA neurons was significantly higher than the percentage of worms with incidences of neuronal loss by Day 11. This discrepancy may be due to the time course of these events. Axonal guidance is an embryonic event and misguided axons remain constant regardless of the worm's age, whereas neuronal loss is progressive with incidences increasing with age. This suggests that DA axonal misguidance may not directly lead to neuronal death in all cases, but could be a contributing factor to the increased neuronal loss.

Another factor that may cause increased neuronal loss could be the enhanced vulnerability of the DA neurons of VAPB-WT and VAPB-P56S strains to oxidative

stress. Oxidative stress is described by an imbalance between biochemical processes, which leads to the production of reactive oxygen species (ROS). Recent research has shown that oxidative stress is widely involved in diseases, especially ones with increased incidence with age. ROS damage all macromolecules in the cell, and the CNS is particularly susceptible to oxidative stress (Sayre et al., 2008). Paraquat is a non-selective, widely used bipyridyl herbicide that is a prototypical agent for experimental generation of ROS (Drechsel and Patel, 2009). The Paraquat treatment protocol was meant to exert an acute oxidative insult to the worms and test the ability of neurons expressing VAPB-WT and VAPB-P56S to withstand and recover from the insult. Both VAPB-WT and VAPB-P56S strains displayed significant increases in the frequency of worms with neuronal loss following Paraquat treatment by Day 3, 7 and 11. In contrast, there was only a minor increase in the control, implying that control DA neurons can tolerate the Paraquat treatment, and that VAPB-WT and VAPB-P56S expression render the DA neurons more vulnerable to oxidative damage or decrease their ability to recover from the oxidative insult. Environmental factors such as oxidative stress, can disrupt ER homeostasis and lead to an accumulation of unfolded or misfolded protein in the ER lumen (Xu et al., 2005). Exposure to oxidative stress activates UPR, which acts as an adaptive mechanism to relieve ER stress and promote cell survival (Malhotra and Kaufman, 2007). However, previous studies have shown that the P56S mutation in a single allele abolishes the ability for VAPB to activate UPR (Kanekura et al., 2006), which could lead to sustained ER stress and subsequent apoptotic cell death. This might explain the enhanced vulnerability of the VAPB-P56S expressing DA neurons to neuronal death, and further characterization of the UPR might provide insights to this

issue.

DA axonal misguidance and neuronal loss may contribute to the backward locomotion defect of VAPB transgenic strains

In addition to axonal misguidance mentioned earlier, DA motor neuronal loss may also contribute to the slowed backward locomotion defect of VAPB-WT and VAPB-P56S strains, since these motor neurons control backward movement and the observed neuronal loss was specific to DA motor neurons. As the worms age, the percentage of VAPB-WT and VAPB-P56S worms with incidences of neuronal loss increased while the rate of backward locomotion decreased. Control worms, which had little to no DA neuronal loss from Day 3 to 11, moved at a faster rate than the transgenic strains. The locomotor defect correlated with the higher frequency of motor neuronal loss in these strains. However, there does not appear to be a direct correlation between VAPB-WT and VAPB-P56S worms since they moved at similar rates backwards despite the higher frequency of VAPB-WT worms with incidences of axonal misguidance and neuronal loss. Taken together, axonal misguidance and neuronal loss could be contributing factors to the locomotor dysfunction, but other factors may modulate this behaviour.

VAPB-WT strains exhibit a possible overexpression phenotype

ALS8 is a familial form of ALS that is characterized by a VAPB-P56S mutation. Previous studies have shown that VAPB-P56S dimerizes with endogenous VAPB-WT and acts in a dominant negative fashion, causing defects in both the ER and nuclear envelope (Kanekura et al., 2006; Prosser et al., 2008; Teuling et al., 2007; Tran et al., 2012). Although expression of VAPB-P56S in DA neurons results in a locomotor defect, increased vulnerability to oxidative stress and premature motor neuronal death, in the axonal misguidance and neuronal loss studies conducted in the VAPB transgenic *C. elegans*, the expression of VAPB-WT appeared to be more detrimental than VAPB-P56S expression. It led to higher frequencies of axonal guidance defects across DA neurons as well as a higher frequency of motor neuronal loss before and after Paraquat treatment. This unexpected finding may be due to an overexpression phenotype. Although only one copy of the VAPB-WT and VAPB-P56S gene was subcloned into the pAC56-*unc-4p* plasmid, by microinjection creation of the transgenic worms, the resulting worms typically carry large extrachromosomal arrays that contain multiple copies of the co-injected DNAs (Evans 2006). The level of expression is very difficult to control and since the number of gene copies can vary, VAPB-WT could be expressed at a much higher level than VAPB-P56S in the DA neurons.

Earlier studies conducted in cells also showed that the overexpression of wild-type VAP has side effects. For example, overexpression of wild-type A isoform (VAPA) inhibited ER-to-Golgi transport of membrane proteins (Prosser et al., 2008). Likewise, the ALS8 *Drosophila* model showed overexpression artifacts with wild-type VAP (Pennetta et al., 2002). Flies with a loss of DVAP-33A displayed motor defects including

a severe decrease in the number of boutons in the muscles of the abdominal segment and a consequent increase in bouton size. However, the overexpression of DVAP-33A resulted in a gain of function, causing an increase in the number of boutons and a decrease in size (Pennetta et al., 2002). Consistent with this, overexpressing VAPB-WT in the DA neurons significantly reduced the lifespan of the *C. elegans* compared to the VAPB-P56S and control (Figure 17). Thus, overexpressing VAPB-WT protein may result in a gain of function that gives rise to the observed phenotype.

vpr-1(RNAi) Knockdown *C. elegans* Model

Based on cellular studies and investigations involving animal models, the general consensus is that the autosomal-dominant ALS8 causing mutant VAPB-P56S is aggregate prone and dimerizes with endogenous VAPB-WT, acting in a dominant negative fashion. Clinical studies have also showed decreased VAPB expression spinal cords of ALS patients (Anagnostou et al., 2010) and motor neurons derived from iPSCs of ALS8 patients (Mitne-Neto et al., 2011). Together, ALS8 is likely caused by a loss of VAPB function. To recapitulate this and to mitigate the overexpression phenotypes associated with the VAPB transgenic *C. elegans* models, a knockdown model of the VAP ortholog in *C. elegans* (*vpr-1*) through RNAi was generated.

RNAi knockdown of *vpr-1* in DA neurons was induced through heat shock, as described in Materials and Methods. The heat shock protocol was designed to minimize the effect of temperature. Previous studies have heat shocked worms at 35°C for 2 to 4 hours (Strayer et al., 2003) but in these heat shock-induced *vpr-1* knockdown experiments, heat shock was limited to 2.5 hours on alternating days so the worms could recover in between.

vpr-1 knockdown in DA neurons results in late-onset uncoordination and slowed rates of backward locomotion

An undulating, sinusoidal propagation of dorsoventral body bends from the posterior to the anterior describes the typical backward-directed locomotion of *C. elegans* following stimulus to its anterior end (Gray et al., 2005). Uncoordination is a common behavioral phenotype where the worm makes a few body bends but comes to a rest in a

coiled posture, forming a spiral, and remains stationary in this position for a period of time. This defect may be the result of a disruption of neuronal input to the body wall and interruption of the typical pattern of alternating waves of contraction along the body wall (Herndon 2009). Following heat shock induced *vpr-1* knockdown in the DA neurons, no significant locomotor defect was observed in young worms (Day 3), but there was a significant increase in the frequency of worms exhibiting uncoordinated backward-directed locomotion in the form of coiling or partial body movements by Day 6 (Figure 22). In addition, there was a significant decline in the rate of backward locomotion in *vpr-1* knocked down worms as well (Figure 20) by Day 6. Notably, heat-shocking the control led to no locomotor defect in terms of uncoordination or declined rates of locomotion. Although there was a general decrease in the rate of backward locomotion as the worms aged, there was no significant increase in the incidences of uncoordination in older worms that did not have *vpr-1* knocked down. The locomotor behavior of control and non-heat shocked *vpr-1(RNAi)* were also very similar in all cases and showed no motor deficit. This suggests that the locomotor defects, uncoordination and slowed rate of backward locomotion, are not only age-dependent but also dependent on the knockdown of *vpr-1*.

vpr-1 knockdown in DA neurons induces age-dependent neuronal loss

Similar to VAPB transgenic strains, the *vpr-1(RNAi)* strains were crossed with an *unc-129p::GFP* reporter strain, which expresses GFP in DA and DB motor neurons as well as weakly in the dorsal muscle cells (Colavita et al., 1998). Since *C. elegans* remain transparent throughout their lifecycle, the axons and cell bodies of the DA and DB motor

neurons were visualized easily under a fluorescence microscope for axonal misguidance and a lack of commissures and cell body was scored as neuronal loss.

vpr-1(RNAi) worms were subject to heat shock 21.5 hours after the embryos were harvested, which induced *vpr-1* knockdown during their L2 stage. This bypassed any issues related to the embryonic lethality of the loss of *vpr-1* in *C. elegans*. Interestingly, axonal misguidance, which was observed in the VAPB transgenic strain with VAPB-WT and VAPB-P56S expression, was not observed in the *vpr-1(RNAi)* strains following *vpr-1* knockdown. This provides further evidence that the previously observed axonal misguidance was a developmental defect as *vpr-1* was knocked down after embryogenesis in this model.

By Day 3 of adulthood following *vpr-1* knockdown, very little neuronal loss was observed in the *vpr-1(RNAi)* strain, similar to the strains that did not have *vpr-1* knocked down. However, a significant increase in the frequency of worms exhibiting neuronal loss was seen by Day 6, specific to the *vpr-1(RNAi)* strain following heat shocked induced *vpr-1* knockdown (Figure 24). This indicates that the loss of DA neurons is not only dependent on the knockdown of *vpr-1* but is also age-dependent.

The age-dependent DA neuronal loss may explain the backward locomotion deficits observed in the *vpr-1(RNAi)* by Day 6 of adulthood. Uncoordination in backward-directed locomotion was not observed until Day 6 of adulthood and similarly, the significant increase in the percentage of worms with DA neuronal loss was observed at Day 6 as well. Although the rate of locomotion in the worms declines with age, the strain with *vpr-1* knocked down slowed significantly, which may also be explained by the significant increase in DA neuronal loss by Day 6. As one or more DA neurons on the

ventral cord die, the lack of innervation of certain segments of the dorsal muscle may be impacting the ability of the worm to make alternating waves of contraction along the body wall for its typical sinusoidal motion, and thus, creating an uncoordinated, slow locomotor deficit.

DA6 and DA7 neurons are the most vulnerable

Of the 113 motor neurons in *C. elegans*, 75 motor neurons innervate the body wall muscle posterior to the head. DA and DB cholinergic motor neurons are classes of motor neurons that are easily visible and are, therefore, often used in worm neuronal studies. These ventral cord motor neurons innervate dorsal muscles by sending commissures to the dorsal side (White et al., 1986). The nine DA motor neurons, with commissures directed towards the anterior end, are responsible for backward locomotion. Meanwhile, the seven DB neurons, with commissures directed towards the posterior end, are responsible for forward locomotion (Figure 8) (White et al., 1976; White et al., 1986). In both the human VAPB transgenic model and the *vpr-1* knockdown model, DA6 and DA7 appear to be the most vulnerable DA neurons (Figure 14, 16, 19, 25). In all studies, including axonal misguidance, oxidative stress and neuronal loss experiments, there was little to no defect observed in the DB neurons controlling forwards locomotion as VAPB-WT and VAPB-P56S were only expressed in the DA neurons. Likewise, *vpr-1* knockdown was specific to DA neurons in the *vpr-1(RNAi)* knockdown model and little DB neuronal loss was observed. Neither models displayed forward-directed locomotor defects as a result. With the highest percentage of defect in these DA neurons, DA6 and DA7 appear to be the most susceptible to age-dependent neuronal loss with or without induction of oxidative stress (as well as axonal misguidance in VAPB-WT strains).

Although increased axonal misguidance in the DA6 and DA7 neurons of VAPB-WT strains may explain the increased age-dependent loss of those mistargeted neurons, there was no obvious specificity in VAPB-P56S worms, which could be further evidence that VAPB-WT defects are overexpression artifacts. On the other hand, DA6 and DA7 were the most vulnerable DA neurons to oxidative stress and age-dependent neuronal loss in the VAPB transgenic worms. Similarly, DA6 and DA7 are also the most susceptible to age-dependent neuronal loss following *vpr-1* knockdown. Located in the posterior end of the *C. elegans*, DA6 and DA7 may be subject to specific environmental factors such as cues or growth factors, which affect the posterior end of the worm and make the neurons more sensitive. However, the exact reason for this bias is unclear. Interestingly, from *C. elegans* network models of known connections of DA6 and DA7 neurons, it is believed that the total lengths of dendritic branches and axons of DA6 and DA7 projecting towards the anterior end are the longest of the class of DA neurons (OpenWorm 2014). It is possible that the longer lengths of DA6 and DA7 neurons render them more vulnerable to age-dependent neuronal loss.

The "dying-back" hypothesis of axon degeneration is that, generally, the most distal portions of axons degenerate first and subsequent axonal atrophy progresses slowly towards the cell body of the neuron. It is believed that motor neurons and nerve terminals may exhibit pathological changes prior to motor neuron degeneration and symptom-onset (Ozturk et al., 2013). Recently, there has been evidence that ALS can be defined as a distal axonopathy (Fischer et al., 2004; Moloney et al., 2014), whereby the distal neuromuscular junctions are affected initially and degeneration then progresses proximally to the neuronal cell body. ALS8 patients in particular experience deep-tendon

reflexes that are common in distal axonopathies (Nishimura et al., 2004b). In addition, histological reports of the "dying-back" phenomena have been documented in a sALS patient with denervation and innervation changes in muscles without evidence of motor neuron death (Fischer et al., 2004), and early changes in distal peripheral nerves have been detected in early muscle weakness through electrophysiological observations (Dengler et al., 1990). Also, longer axons equate to further transport of proteins and necessary factors from the cell body to the axons and dendrites. As a result, possible ER-trafficking defects associated with VAPB-P56S mutation or loss of VAPB could affect transport to the distal ends significantly. Signals and proteins need to traverse dendrites and axons and efficient regulation is vital to neuronal plasticity and survival (Bito and Takemoto-Kimura, 2003). Consequently, it is possible that, if the distal portions of axons are more susceptible to degeneration, the longer axons in DA6 and DA7 neurons could more sensitive to damage and subsequent "dying-back", especially with the expression of VAPB-P56S or a loss of VPR-1.

vpr-1 knockdown or VAPB-P56S induced neuronal loss in DA neurons may be due to multiple factors such as ER and nuclear envelope defects

Despite their autosomal dominant hereditary background, ALS8 patients do not experience ALS symptoms and are not diagnosed until they are between 25-55 years old. Since the current view of the pathogenesis of VAPB-P56S is a loss of function mutation that causes ALS8, it was not unexpected to find that expression of VAPB-P56S in the DA neurons as well as the knockdown of *vpr-1* both induced locomotor deficits and age-dependent neuronal loss. The age-dependent neuronal loss in ALS8 cases may be explained by multiple factors. Investigations have shown that the expression of VAPB-

P56S causes two main changes to the cell that lead to the loss of the characteristic reticular structure of the ER, resulting in an ER defect, as well as the deterioration of the nuclear envelope and subsequent nuclear envelope defect. Both defects may contribute to neurodegeneration. VAPB-P56S is highly aggregate-prone and able to dimerize and sequester VAPB-WT into its cytoplasmic inclusions, acting in a dominant negative fashion. VAPB-P56S attenuates the activation of IRE1/XBP1 pathway, one of the main pathways of the unfolded protein response (UPR) (Suzuki et al., 2009). UPR is a physiological reaction that prevents the accumulation of unfolded and misfolded proteins in the ER and restores ER function. However, with the reduction of VAPB, UPR is not activated, which may also explain the increased vulnerability of the VAPB-P56S expressing DA neurons to oxidative stress. Without UPR, protein aggregation builds up within the cell, interrupting neuronal function and possibly contributing to ER-stress induced neuronal death (Kanekura et al., 2006).

Additionally, neuronal loss may be attributed to VAPB-P56S causing a nuclear envelope defect that leads to essential nuclear envelope and pore proteins to "leak out" and remain in the cytoplasm. Previous cell studies showed that VAPB-P56S caused a dilated or "herniated" nuclear envelope and nuclear membrane proteins and nucleoporins, building blocks of the nuclear pore complex, such as gp-210, and emerin, were retained in the mutant VAPB aggregates. siRNA knockdown of endogenous VAPB exhibit similar phenotypes, which suggests that the cytoplasmic retention of these nuclear proteins is due to a loss of VAPB function (Tran et al., 2012) and could also be happening in the *vpr-1* knockdown model. Progressive deterioration of the nuclear envelope is an ageing phenomenon, as exemplified by progeria due to Lamin A mutation (Worman, 2012).

Therefore, the progressive deterioration of the nuclear envelope and altered morphology may also be a contributing factor to neuronal loss and the age-dependent onset of disease. Because neurons are highly polarized, bidirectional trafficking of proteins between the cytoplasm and nucleus is essential for signal transduction and neuronal survival (Patel and Chu, 2011). Any disruption of efficient nucleocytoplasmic transport caused by defects linked to VAPB-P56S or *vpr-1* knockdown could impair neuronal function and subsequently, prolonged inefficiency could lead to neurodegeneration.

The two-hit hypothesis has also been used to explain the age-dependent onset of disease symptoms (Vance et al., 2013). In this scenario, a second hit is needed to trigger neuronal death. Expression of mutant VAPB or knockdown of endogenous VAPB expression (VPR-1 in *C. elegans*) may disrupt cellular functions that then render neurons more vulnerable to mild external insults. This would lead to premature loss of neurons, as seen with Paraquat treatment of VAPB transgenic worms. Thus, the cumulative effect of stressors and other factors could modulate the onset and progression of motor neuron degeneration.

Future Direction

The *vpr-1(RNAi)* knockdown model circumvented the overexpression phenotype associated with the human VAPB transgenic model and is the better of the two models for ALS8 going forward. Future studies that may be conducted include looking at later stages of the lifecycle, assessing the vulnerability of the DA neurons following *vpr-1* knockdown to oxidative stress, as well as determining the underlying mechanism causing neuronal death. For example, a hallmark of sALS and fALS is the mislocalization of

nuclear protein TAR-DNA binding protein-43 (TDP-43) to inclusions in the cytoplasm (Anagnostou et al., 2010), which may be a nuclear envelope defect that could be assessed in the *vpr-1* knockdown model. Future investigations on the effect of *vpr-1* knockdown on the nuclear envelope could be evaluated by injecting a construct expressing a nuclear protein, such as TDP-43, tagged with a red fluorescent protein to allow visualization of the protein localization and analyze whether the nuclear protein is sequestered in the cytoplasm like human ALS cases. Determining the basic biological function of the VAP ortholog, VPR-1, in *C. elegans*, could provide insight on the function of VAPB and the molecular mechanisms by which VAPB-P56S affects and causes motor neuronal death in human cases of ALS8. Furthermore, this *vpr-1(RNAi) C. elegans* model would also be useful for high-throughput drug screening to test drugs or other treatments that can delay the onset of neuronal death in ALS8.

REFERENCES

Al-Chalabi, A., and O. Hardiman. 2013. The epidemiology of ALS: a conspiracy of genes, environment and time. *Nature reviews. Neurology*. 9:617-628.

Aliaga, L., C. Lai, J. Yu, N. Chub, H. Shim, L. Sun, C. Xie, W.J. Yang, X. Lin, M.J. O'Donovan, and H. Cai. 2013. Amyotrophic lateral sclerosis-related VAPB P56S mutation differentially affects the function and survival of corticospinal and spinal motor neurons. *Human molecular genetics*. 22:4293-4305.

Anagnostou, G., M.T. Akbar, P. Paul, C. Angelinetta, T.J. Steiner, and J. de Belleroche. 2010. Vesicle associated membrane protein B (VAPB) is decreased in ALS spinal cord. *Neurobiology of aging*. 31:969-985.

Andrade, J., H. Zhao, B. Titus, S. Timm Pearce, and M. Barroso. 2004. The EF-hand Ca2+-binding protein p22 plays a role in microtubule and endoplasmic reticulum organization and dynamics with distinct Ca2+-binding requirements. *Molecular biology of the cell*. 15:481-496.

Asikainen, S., S. Vartiainen, M. Lakso, R. Nass, and G. Wong. 2005. Selective sensitivity of Caenorhabditis elegans neurons to RNA interference. *Neuroreport*. 16:1995-1999.

Avery, L. and You, Y.J. *C. elegans* feeding (May 21, 2012), *WormBook*, ed. The *C. elegans* Research Community, WormBook, doi/10.1895/wormbook.1.150.1, http://www.wormbook.org.

Baker, A.M., T.M. Roberts, and M. Stewart. 2002. 2.6 A resolution crystal structure of helices of the motile major sperm protein (MSP) of Caenorhabditis elegans. *Journal of molecular biology*. 319:491-499.

Bito, H., and S. Takemoto-Kimura. 2003. Ca(2+)/CREB/CBP-dependent gene regulation: a shared mechanism critical in long-term synaptic plasticity and neuronal survival. *Cell calcium*. 34:425-430.

Boillee, S., C. Vande Velde, and D.W. Cleveland. 2006. ALS: a disease of motor neurons and their nonneuronal neighbors. *Neuron*. 52:39-59.

Bottino, D., A. Mogilner, T. Roberts, M. Stewart, and G. Oster. 2002. How nematode sperm crawl. *Journal of cell science*. 115:367-384.

Brenner, S. 1974. The genetics of Caenorhabditis elegans. *Genetics*. 77:71-94.

Caldicott, I.M., Larsen, P.L., and Riddle, D.L. (1994). In: *Cell biology: a laboratory handbook*. (San Diego: Academic Press), pp. 389.

Chai, A., J. Withers, Y.H. Koh, K. Parry, H. Bao, B. Zhang, V. Budnik, and G. Pennetta. 2008. hVAPB, the causative gene of a heterogeneous group of motor neuron diseases in humans, is functionally interchangeable with its Drosophila homologue DVAP-33A at the neuromuscular junction. *Human molecular genetics*. 17:266-280.

Chio, A., G. Logroscino, O. Hardiman, R. Swingler, D. Mitchell, E. Beghi, B.G. Traynor, and C. Eurals. 2009. Prognostic factors in ALS: A critical review. *Amyotrophic lateral sclerosis : official publication of the World Federation of Neurology Research Group on Motor Neuron Diseases*. 10:310-323.

Colavita, A., S. Krishna, H. Zheng, R.W. Padgett, and J.G. Culotti. 1998. Pioneer axon guidance by UNC-129, a C. elegans TGF-beta. *Science*. 281:706-709.

Dengler, R., A. Konstanzer, G. Kuther, S. Hesse, W. Wolf, and A. Struppler. 1990. Amyotrophic lateral sclerosis: macro-EMG and twitch forces of single motor units. *Muscle & nerve*. 13:545-550.

Dorst, J., P. Kuhnlein, C. Hendrich, J. Kassubek, A.D. Sperfeld, and A.C. Ludolph. 2011. Patients with elevated triglyceride and cholesterol serum levels have a prolonged survival in amyotrophic lateral sclerosis. *Journal of neurology*. 258:613-617.

Drechsel, D.A., and M. Patel. 2009. Chapter 21 Paraquat-induced production of reactive oxygen species in brain mitochondria. *Methods in enzymology*. 456:381-393.

Dupuis, L., P. Corcia, A. Fergani, J.L. Gonzalez De Aguilar, D. Bonnefont-Rousselot, R. Bittar, D. Seilhean, J.J. Hauw, L. Lacomblez, J.P. Loeffler, and V. Meininger. 2008. Dyslipidemia is a protective factor in amyotrophic lateral sclerosis. *Neurology*. 70:1004-1009.

Dupuis, L., P.F. Pradat, A.C. Ludolph, and J.P. Loeffler. 2011. Energy metabolism in amyotrophic lateral sclerosis. *The Lancet. Neurology*. 10:75-82.

Esmaeili, B., J.M. Ross, C. Neades, D.M. Miller, 3rd, and J. Ahringer. 2002. The C. elegans even-skipped homologue, vab-7, specifies DB motoneurone identity and axon trajectory. *Development*. 129:853-862.

Evans, T. C., ed. Transformation and microinjection (April 6, 2006), *WormBook*, ed. The *C. elegans* Research Community, WormBook, doi/10.1895/wormbook.1.108.1, http://www.wormbook.org.

Fay, D. Genetic mapping and manipulation: Chapter 7-Making compound mutants (February 17, 2006), *WormBook*, ed. The *C. elegans* Research Community, WormBook, doi/10.1895/wormbook.1.96.1, http://www.wormbook.org.

Fire, A., S. Xu, M.K. Montgomery, S.A. Kostas, S.E. Driver, and C.C. Mello. 1998. Potent and specific genetic interference by double-stranded RNA in Caenorhabditis elegans. *Nature*. 391:806-811.

Fischer, L.R., D.G. Culver, P. Tennant, A.A. Davis, M. Wang, A. Castellano-Sanchez, J. Khan, M.A. Polak, and J.D. Glass. 2004. Amyotrophic lateral sclerosis is a distal axonopathy: evidence in mice and man. *Experimental neurology*. 185:232-240.

Funke, A.D., M. Esser, A. Kruttgen, J. Weis, M. Mitne-Neto, M. Lazar, A.L. Nishimura, A.D. Sperfeld, P. Trillenberg, J. Senderek, M. Krasnianski, M. Zatz, S. Zierz, and M. Deschauer. 2010. The p.P56S mutation in the VAPB gene is not due to a single founder: the first European case. *Clinical genetics*. 77:302-303.

Furuita, K., J. Jee, H. Fukada, M. Mishima, and C. Kojima. 2010. Electrostatic interaction between oxysterol-binding protein and VAMP-associated protein A revealed by NMR and mutagenesis studies. *The Journal of biological chemistry*. 285:12961-12970.

Gordon, P.H. 2013. Amyotrophic Lateral Sclerosis: An update for 2013 Clinical Features, Pathophysiology, Management and Therapeutic Trials. *Aging and disease*. 4:295-310.

Gray, J., and H.W. Lissmann. 1964. The Locomotion of Nematodes. *The Journal of experimental biology*. 41:135-154.

Gray, J.M., J.J. Hill, and C.I. Bargmann. 2005. A circuit for navigation in Caenorhabditis elegans. *Proceedings of the National Academy of Sciences of the United States of America*. 102:3184-3191.

Han, S.M., H. El Oussini, J. Scekic-Zahirovic, J. Vibbert, P. Cottee, J.K. Prasain, H.J. Bellen, L. Dupuis, and M.A. Miller. 2013. VAPB/ALS8 MSP ligands regulate striated muscle energy metabolism critical for adult survival in caenorhabditis elegans. *PLoS genetics*. 9:e1003738.

Hart, Anne C., ed. Behavior (July 3, 2006), *WormBook*, ed. The *C. elegans* Research Community, WormBook, doi/10.1895/wormbook.1.87.1, http://www.wormbook.org.

Herndon, L.A., Altun, Z.F. and Hall, D.H. 2009. Glossary C. In *WormAtlas*. doi:10.3908/wormatlas.6.3

Jorgensen, E.M., and S.E. Mango. 2002. The art and design of genetic screens: caenorhabditis elegans. *Nature reviews. Genetics*. 3:356-369.

Kabashi, E., H. El Oussini, V. Bercier, F. Gros-Louis, P.N. Valdmanis, J. McDearmid, I.A. Mejier, P.A. Dion, N. Dupre, D. Hollinger, J. Sinniger, S. Dirrig-Grosch, W. Camu, V. Meininger, J.P. Loeffler, F. Rene, P. Drapeau, G.A. Rouleau, and L.

Dupuis. 2013. Investigating the contribution of VAPB/ALS8 loss of function in amyotrophic lateral sclerosis. *Human molecular genetics*. 22:2350-2360.

Kaletta, T., and M.O. Hengartner. 2006. Finding function in novel targets: C. elegans as a model organism. *Nature reviews. Drug discovery*. 5:387-398.

Kamath, R.S., A.G. Fraser, Y. Dong, G. Poulin, R. Durbin, M. Gotta, A. Kanapin, N. Le Bot, S. Moreno, M. Sohrmann, D.P. Welchman, P. Zipperlen, and J. Ahringer. 2003. Systematic functional analysis of the Caenorhabditis elegans genome using RNAi. *Nature*. 421:231-237.

Kanekura, K., I. Nishimoto, S. Aiso, and M. Matsuoka. 2006. Characterization of amyotrophic lateral sclerosis-linked P56S mutation of vesicle-associated membrane protein-associated protein B (VAPB/ALS8). *The Journal of biological chemistry*. 281:30223-30233.

Kawano, M., K. Kumagai, M. Nishijima, and K. Hanada. 2006. Efficient trafficking of ceramide from the endoplasmic reticulum to the Golgi apparatus requires a VAMP-associated protein-interacting FFAT motif of CERT. *The Journal of biological chemistry*. 281:30279-30288.

Kenyon, C. 1988. The nematode Caenorhabditis elegans. *Science*. 240:1448-1453.

Kim, I., W. Xu, and J.C. Reed. 2008. Cell death and endoplasmic reticulum stress: disease relevance and therapeutic opportunities. *Nature reviews. Drug discovery*. 7:1013-1030.

Kim, S., S.S. Leal, D. Ben Halevy, C.M. Gomes, and S. Lev. 2010. Structural requirements for VAP-B oligomerization and their implication in amyotrophic lateral sclerosis-associated VAP-B(P56S) neurotoxicity. *The Journal of biological chemistry*. 285:13839-13849.

Klein, R. 2004. Eph/ephrin signaling in morphogenesis, neural development and plasticity. *Current opinion in cell biology*. 16:580-589.

Kuhnlein, P., H.J. Gdynia, A.D. Sperfeld, B. Lindner-Pfleghar, A.C. Ludolph, M. Prosiegel, and A. Riecker. 2008. Diagnosis and treatment of bulbar symptoms in amyotrophic lateral sclerosis. *Nature clinical practice. Neurology*. 4:366-374.

Kuijpers, M., V. van Dis, E.D. Haasdijk, M. Harterink, K. Vocking, J.A. Post, W. Scheper, C.C. Hoogenraad, and D. Jaarsma. 2013. Amyotrophic lateral sclerosis (ALS)-associated VAPB-P56S inclusions represent an ER quality control compartment. *Acta neuropathologica communications*. 1:24.

Kumar, D.R., F. Aslinia, S.H. Yale, and J.J. Mazza. 2011. Jean-Martin Charcot: the father of neurology. *Clinical medicine & research*. 9:46-49.

Kurland, L.T., and D.W. Mulder. 1955a. Epidemiologic investigations of amyotrophic lateral sclerosis. 2. Familial aggregations indicative of dominant inheritance. I. *Neurology*. 5:182-196.

Kurland, L.T., and D.W. Mulder. 1955b. Epidemiologic investigations of amyotrophic lateral sclerosis. 2. Familial aggregations indicative of dominant inheritance. II. *Neurology*. 5:249-268.

Leroux, M.R., R. Melki, B. Gordon, G. Batelier, and E.P. Candido. 1997. Structure-function studies on small heat shock protein oligomeric assembly and interaction with unfolded polypeptides. *The Journal of biological chemistry*. 272:24646-24656.

Lev, S. 2004. The role of the Nir/rdgB protein family in membrane trafficking and cytoskeleton remodeling. *Experimental cell research*. 297:1-10.

Levine, T.P., and S. Munro. 2001. Dual targeting of Osh1p, a yeast homologue of oxysterol-binding protein, to both the Golgi and the nucleus-vacuole junction. *Molecular biology of the cell*. 12:1633-1644.

Lewis, J.A., and J.T. Fleming. 1995. Basic culture methods. *Methods in cell biology*. 48:3-29.

Lewis, J.A., C.H. Wu, H. Berg, and J.H. Levine. 1980. The genetics of levamisole resistance in the nematode Caenorhabditis elegans. *Genetics*. 95:905-928.

Lickteig, K.M., J.S. Duerr, D.L. Frisby, D.H. Hall, J.B. Rand, and D.M. Miller, 3rd. 2001. Regulation of neurotransmitter vesicles by the homeodomain protein UNC-4 and its transcriptional corepressor UNC-37/groucho in Caenorhabditis elegans cholinergic motor neurons. *The Journal of neuroscience : the official journal of the Society for Neuroscience*. 21:2001-2014.

Loewen, C.J., A. Roy, and T.P. Levine. 2003. A conserved ER targeting motif in three families of lipid binding proteins and in Opi1p binds VAP. *The EMBO journal*. 22:2025-2035.

Malhotra, J.D., and R.J. Kaufman. 2007. Endoplasmic reticulum stress and oxidative stress: a vicious cycle or a double-edged sword? *Antioxidants & redox signaling*. 9:2277-2293.

Mello, C.C., J.M. Kramer, D. Stinchcomb, and V. Ambros. 1991. Efficient gene transfer in C.elegans: extrachromosomal maintenance and integration of transforming sequences. *The EMBO journal*. 10:3959-3970.

Millecamps, S., F. Salachas, C. Cazeneuve, P. Gordon, B. Bricka, A. Camuzat, L. Guillot-Noel, O. Russaouen, G. Bruneteau, P.F. Pradat, N. Le Forestier, N. Vandenberghe, V. Danel-Brunaud, N. Guy, C. Thauvin-Robinet, L. Lacomblez, P. Couratier, D. Hannequin, D. Seilhean, I. Le Ber, P. Corcia, W. Camu, A. Brice,

G. Rouleau, E. LeGuern, and V. Meininger. 2010. SOD1, ANG, VAPB, TARDBP, and FUS mutations in familial amyotrophic lateral sclerosis: genotype-phenotype correlations. *Journal of medical genetics*. 47:554-560.

Miller, D.M., M.M. Shen, C.E. Shamu, T.R. Burglin, G. Ruvkun, M.L. Dubois, M. Ghee, and L. Wilson. 1992. C. elegans unc-4 gene encodes a homeodomain protein that determines the pattern of synaptic input to specific motor neurons. *Nature*. 355:841-845.

Miller, M.A., V.Q. Nguyen, M.H. Lee, M. Kosinski, T. Schedl, R.M. Caprioli, and D. Greenstein. 2001. A sperm cytoskeletal protein that signals oocyte meiotic maturation and ovulation. *Science*. 291:2144-2147.

Miller, M.A., P.J. Ruest, M. Kosinski, S.K. Hanks, and D. Greenstein. 2003. An Eph receptor sperm-sensing control mechanism for oocyte meiotic maturation in Caenorhabditis elegans. *Genes & development*. 17:187-200.

Mitne-Neto, M., M. Machado-Costa, M.C. Marchetto, M.H. Bengtson, C.A. Joazeiro, H. Tsuda, H.J. Bellen, H.C. Silva, A.S. Oliveira, M. Lazar, A.R. Muotri, and M. Zatz. 2011. Downregulation of VAPB expression in motor neurons derived from induced pluripotent stem cells of ALS8 patients. *Human molecular genetics*. 20:3642-3652.

Moloney, E.B., F. de Winter, and J. Verhaagen. 2014. ALS as a distal axonopathy: molecular mechanisms affecting neuromuscular junction stability in the presymptomatic stages of the disease. *Frontiers in neuroscience*. 8:252.

Nishimura, A.L., M. Mitne-Neto, H.C. Silva, J.R. Oliveira, M. Vainzof, and M. Zatz. 2004a. A novel locus for late onset amyotrophic lateral sclerosis/motor neurone disease variant at 20q13. *Journal of medical genetics*. 41:315-320.

Nishimura, A.L., M. Mitne-Neto, H.C. Silva, A. Richieri-Costa, S. Middleton, D. Cascio, F. Kok, J.R. Oliveira, T. Gillingwater, J. Webb, P. Skehel, and M. Zatz. 2004b. A mutation in the vesicle-trafficking protein VAPB causes late-onset spinal muscular atrophy and amyotrophic lateral sclerosis. *American journal of human genetics*. 75:822-831.

Nishimura, Y., M. Hayashi, H. Inada, and T. Tanaka. 1999. Molecular cloning and characterization of mammalian homologues of vesicle-associated membrane protein-associated (VAMP-associated) proteins. *Biochemical and biophysical research communications*. 254:21-26.

OpenWorm. "*C. elegans* Network Model." *Opensource Brain.* 2014. Web. 23 Jan. 2015. <http://www.opensourcebrain.org/embedded/celegans/index.html>.

Ozturk, G., N. Cengiz, E. Erdogan, A. Him, E.K. Oguz, E. Yenidunya, and N. Aysit. 2013. Two distinct types of dying back axonal degeneration in vitro. *Neuropathology and applied neurobiology*. 39:362-376.

Palmer, A., and R. Klein. 2003. Multiple roles of ephrins in morphogenesis, neuronal networking, and brain function. *Genes & development*. 17:1429-1450.

Park, S.K., P.M. Tedesco, and T.E. Johnson. 2009. Oxidative stress and longevity in Caenorhabditis elegans as mediated by SKN-1. *Aging cell*. 8:258-269.

Patel, V.P., and C.T. Chu. 2011. Nuclear transport, oxidative stress, and neurodegeneration. *International journal of clinical and experimental pathology*. 4:215-229.

Pennetta, G., P.R. Hiesinger, R. Fabian-Fine, I.A. Meinertzhagen, and H.J. Bellen. 2002. Drosophila VAP-33A directs bouton formation at neuromuscular junctions in a dosage-dependent manner. *Neuron*. 35:291-306.

Prosser, D.C., D. Tran, P.Y. Gougeon, C. Verly, and J.K. Ngsee. 2008. FFAT rescues VAPA-mediated inhibition of ER-to-Golgi transport and VAPB-mediated ER aggregation. *Journal of cell science*. 121:3052-3061.

Ratnaparkhi, A., G.M. Lawless, F.E. Schweizer, P. Golshani, and G.R. Jackson. 2008. A Drosophila model of ALS: human ALS-associated mutation in VAP33A suggests a dominant negative mechanism. *PloS one*. 3:e2334.

Riddle, D.L., T. Blumenthal, B.J. Meyer, and J.R. Priess. 1997. Introduction to C. elegans. *In* C. elegans II. D.L. Riddle, T. Blumenthal, B.J. Meyer, and J.R. Priess, editors, Cold Spring Harbor (NY).

Rohner, S., V. Kalck, X. Wang, K. Ikegami, J.D. Lieb, S.M. Gasser, and P. Meister. 2013. Promoter- and RNA polymerase II-dependent hsp-16 gene association with nuclear pores in Caenorhabditis elegans. *The Journal of cell biology*. 200:589-604.

Ron, D., and P. Walter. 2007. Signal integration in the endoplasmic reticulum unfolded protein response. *Nature reviews. Molecular cell biology*. 8:519-529.

Sayre, L.M., G. Perry, and M.A. Smith. 2008. Oxidative stress and neurotoxicity. *Chemical research in toxicology*. 21:172-188.

Skehel, P.A., K.C. Martin, E.R. Kandel, and D. Bartsch. 1995. A VAMP-binding protein from Aplysia required for neurotransmitter release. *Science*. 269:1580-1583.

Strayer, A., Z. Wu, Y. Christen, C.D. Link, and Y. Luo. 2003. Expression of the small heat-shock protein Hsp16-2 in Caenorhabditis elegans is suppressed by Ginkgo biloba extract EGb 761. *FASEB journal : official publication of the Federation of American Societies for Experimental Biology*. 17:2305-2307.

Sulston, J.E., and H.R. Horvitz. 1977. Post-embryonic cell lineages of the nematode, Caenorhabditis elegans. *Developmental biology*. 56:110-156.

Sulston, J.E., E. Schierenberg, J.G. White, and J.N. Thomson. 1983. The embryonic cell lineage of the nematode Caenorhabditis elegans. *Developmental biology*. 100:64-119.

Sutphin, G.L., and M. Kaeberlein. 2009. Measuring Caenorhabditis elegans life span on solid media. *Journal of visualized experiments : JoVE*.

Suzuki, H., K. Kanekura, T.P. Levine, K. Kohno, V.M. Olkkonen, S. Aiso, and M. Matsuoka. 2009. ALS-linked P56S-VAPB, an aggregated loss-of-function mutant of VAPB, predisposes motor neurons to ER stress-related death by inducing aggregation of co-expressed wild-type VAPB. *Journal of neurochemistry*. 108:973-985.

Tabara, H., A. Grishok, and C.C. Mello. 1998. RNAi in C. elegans: soaking in the genome sequence. *Science*. 282:430-431.

Tarr, D.E., and A.L. Scott. 2005. MSP domain proteins. *Trends in parasitology*. 21:224-231.

Teuling, E., S. Ahmed, E. Haasdijk, J. Demmers, M.O. Steinmetz, A. Akhmanova, D. Jaarsma, and C.C. Hoogenraad. 2007. Motor neuron disease-associated mutant vesicle-associated membrane protein-associated protein (VAP) B recruits wild-type VAPs into endoplasmic reticulum-derived tubular aggregates. *The Journal of neuroscience : the official journal of the Society for Neuroscience*. 27:9801-9815.

Timmons, L., and A. Fire. 1998. Specific interference by ingested dsRNA. *Nature*. 395:854.

Tran, D., A. Chalhoub, A. Schooley, W. Zhang, and J.K. Ngsee. 2012. A mutation in VAPB that causes amyotrophic lateral sclerosis also causes a nuclear envelope defect. *Journal of cell science*. 125:2831-2836.

Tsuda, H., S.M. Han, Y. Yang, C. Tong, Y.Q. Lin, K. Mohan, C. Haueter, A. Zoghbi, Y. Harati, J. Kwan, M.A. Miller, and H.J. Bellen. 2008. The amyotrophic lateral sclerosis 8 protein VAPB is cleaved, secreted, and acts as a ligand for Eph receptors. *Cell*. 133:963-977.

Tudor, E.L., C.M. Galtrey, M.S. Perkinton, K.F. Lau, K.J. De Vos, J.C. Mitchell, S. Ackerley, T. Hortobagyi, E. Vamos, P.N. Leigh, C. Klasen, D.M. McLoughlin, C.E. Shaw, and C.C. Miller. 2010a. Amyotrophic lateral sclerosis mutant vesicle-associated membrane protein-associated protein-B transgenic mice develop TAR-DNA-binding protein-43 pathology. *Neuroscience*. 167:774-785.

Tudor, E.L., C.M. Galtrey, M.S. Perkinton, K.F. Lau, K.J. de Vos, J.C. Mitchell, S. Ackerley, T. Hortobágyi, E. Vámos, P.N. Leigh, C. Klasen, D.M. McLoughlin, C.E. Shaw, and C.C.J. Miller. 2010b. Amyotrophic lateral sclerosis mutant vesicle-associated membrane protein-associated protein-B transgenic mice develop TAR-DNA-binding protein-43 pathology. *Neuroscience*. 167:774-785.

Turner, M.R., A. Brockington, J. Scaber, H. Hollinger, R. Marsden, P.J. Shaw, and K. Talbot. 2010. Pattern of spread and prognosis in lower limb-onset ALS. *Amyotrophic lateral sclerosis : official publication of the World Federation of Neurology Research Group on Motor Neuron Diseases*. 11:369-373.

Uchikubo, Y., T. Hasegawa, S. Mitani, H.S. Kim, and Y. Wataya. 2002. Mechanisms of cell death induced by 5-fluoro-2'-deoxyuridine (FUdR)--necrosis or apoptosis after treated with FUdR. *Nucleic acids research. Supplement*:245-246.

Vance, C., E.L. Scotter, A.L. Nishimura, C. Troakes, J.C. Mitchell, C. Kathe, H. Urwin, C. Manser, C.C. Miller, T. Hortobagyi, M. Dragunow, B. Rogelj, and C.E. Shaw. 2013. ALS mutant FUS disrupts nuclear localization and sequesters wild-type FUS within cytoplasmic stress granules. *Human molecular genetics*. 22:2676-2688.

White, J.G., E. Southgate, J.N. Thomson, and S. Brenner. 1976. The structure of the ventral nerve cord of Caenorhabditis elegans. *Philosophical transactions of the Royal Society of London. Series B, Biological sciences*. 275:327-348.

White, J.G., E. Southgate, J.N. Thomson, and S. Brenner. 1986. The structure of the nervous system of the nematode Caenorhabditis elegans. *Philosophical transactions of the Royal Society of London. Series B, Biological sciences*. 314:1-340.

Worman, H.J. 2012. Nuclear lamins and laminopathies. *The Journal of pathology*. 226:316-325.

Wyles, J.P., C.R. McMaster, and N.D. Ridgway. 2002. Vesicle-associated membrane protein-associated protein-A (VAP-A) interacts with the oxysterol-binding protein to modify export from the endoplasmic reticulum. *The Journal of biological chemistry*. 277:29908-29918.

Xu, C., B. Bailly-Maitre, and J.C. Reed. 2005. Endoplasmic reticulum stress: cell life and death decisions. *The Journal of clinical investigation*. 115:2656-2664.

Zallen, J.A., S.A. Kirch, and C.I. Bargmann. 1999. Genes required for axon pathfinding and extension in the C. elegans nerve ring. *Development*. 126:3679-3692.

APPENDIX A: BACKWARD LOCOMOTION VIDEO OF DAY 6 *vpr-1(RNAi)* KNOCKDOWN MODEL

Videos are accessible by the attached CD-ROM.

Non-heat shocked and heat shocked control worms display normal sinusoidal backward-directed locomotion. Non-heat shocked *vpr-1(RNAi)* worms also exhibit typical backward locomotion. However, heat shocked *vpr-1(RNAi)* worms are uncoordinated and have a significantly slower rate of backward locomotion. Videos 1-4 show backward-directed locomotion of Adult Day 6 *vpr-1(RNAi)* knockdown model worms following a prod to the anterior end of each worm. The following worms were recorded:

1. Control Non-heat shocked
   (File name: vid1-day6-control-NonHeatshock-16x-WZhang)

2. Control Heat shocked
   (File name: vid2-day6-control-Heatshock-50x-WZhang)

3. *vpr-1(RNAi)* Non-heat shocked
   (File name: vid3-day6-vpr-1(RNAi)-NonHeatShock-16x-WZhang)

4. *vpr-1(RNAi)* Heat shocked
   (File name: vid4-day6-vpr-1(RNAi)-Heatshock-50x-WZhang)

Videos are taken using screen-capture of live brightfield imaging on Zeiss Stereo Discovery.V20 Microscope on a 1x objective. 16x magnification was used to visualize non-heat shocked worms and 50x magnification was used to visualize heat shocked worms.